

St. John's University

St. John's Scholar

Theses and Dissertations

2023

**MEASUREMENT OF DESMOSINE BY LIQUID
CHROMATOGRAPHY–TANDEM MASS SPECTROMETRY AND ITS
APPLICATION TO CHRONIC OBSTRUCTIVE PULMONARY
DISEASE**

Michael Fagiola

Follow this and additional works at: https://scholar.stjohns.edu/theses_dissertations

MEASUREMENT OF DESMOSINE BY LIQUID CHROMATOGRAPHY–TANDEM
MASS SPECTROMETRY AND ITS APPLICATION TO CHRONIC
OBSTRUCTIVE PULMONARY DISEASE

A dissertation submitted in partial fulfillment
of the requirements for the degree of

DOCTOR OF PHILOSOPHY

to the faculty of the

DEPARTMENT OF PHARMACEUTICAL SCIENCES

of

COLLEGE OF PHARMACY AND HEALTH SCIENCES

at

ST. JOHN'S UNIVERSITY

New York

by

Michael Fagiola

Date Submitted: _____

Date Approved: _____

Michael Fagiola

Dr. Jerome Cantor

© Copyright by Michael Fagiola 2023
All Rights Reserved

ABSTRACT

MEASUREMENT OF DESMOSINE BY LIQUID CHROMATOGRAPHY–TANDEM MASS SPECTROMETRY AND ITS APPLICATION TO CHRONIC OBSTRUCTIVE PULMONARY DISEASE

Michael Fagiola

The mechanical properties of lung elastic fibers are derived from the specialized features of their core elastin protein, which contains distensible, coiled peptides that store the energy needed to expel air from the lungs. Elastin crosslinks provide structural support for the fibers and play an important role in determining the morphologic features of the lung. Degradation of elastic fibers in lung disease is associated with the release of desmosine, a unique amino acid that can be readily identified and quantified in body fluids and solid tissue using LC–MS-MS. The purpose of this study was to explore the role of desmosine as a biomarker for emphysematous changes in both animal and human models of COPD.

Female Golden Syrian hamsters were exposed to either secondhand cigarette smoke or normal room air for 4 hours a day over a period of 3 days. 24 hours following exposure, hamsters were injected intraperitoneally with either 200 µg lipopolysaccharide injections in 0.1 mL saline or saline alone. Following euthanasia, hamster lung tissue was collected and evaluated for desmosine content and airspace enlargement. Hamster BALF was also collected and assessed for leukocyte and neutrophil content.

Human lung tissue was collected postmortem from decedents with or without a clinical history of lung disease. This tissue was then evaluated for desmosine content and airspace enlargement. In addition to these studies, authentic human plasma, urine, and sputum samples collected from a previous clinical trial were evaluated for desmosine

content. Desmosine content from both human and hamster models of COPD were measured using a novel LC–MS-MS technique that was developed for the quantification of desmosine in body fluids and solid tissue simultaneously.

Significant increases in desmosine content and airspace enlargement were seen in the lungs of hamsters exposed to cigarette smoke and lipopolysaccharide. BALF leukocytes and neutrophils were concomitantly increased in this exposure group. Similar increases in desmosine content and airspace enlargement were seen in the lungs of human decedents with COPD. Based on these morphological and biochemical findings, desmosine is a sensitive indicator of alveolar wall injury and elastic fiber degradation in COPD.

ACKNOWLEDGMENTS

“I used to live in a room full of mirrors; all I could see was me. I take my spirit and I smash my mirrors, and now the whole world is here for me to see.”

– James Marshall Hendrix (1942-1970)

This minor section of my thesis was actually the longest in writing. This period of academic and scientific growth that culminated in this document was abundant in unforeseen challenges as well as opportunities. This journey’s successful completion would not have been possible without the tireless efforts, unconditional support, and wisdom of many individuals to whom I am exceedingly grateful.

First and foremost, I would like to thank my principal advisor and esteemed mentor, Dr. Jerome O. Cantor. Your steadfast guidance has not only helped shape the work culminating in this thesis, but also the scientist I am today. Under your leadership I improved as a researcher, as a presenter, and as a writer. Good science can be hard and frustrating, yet rewarding and exciting at the same time; through this experience you learn more on the journey than you do at its finish. You not only placed immense confidence in my ability to independently take this project from start to finish, offering advice and wisdom whenever it was needed, but also encouraged me to fully immerse myself within the journey that is earning a Ph.D. in the sciences. Being a part of your lab

has been an absolute pleasure, and I will always remember this experience with pride and gratitude.

I also need to thank my first mentor, Dr. Joseph Avella. You were the person who gave me my start in toxicology and who challenged me to pursue a Ph.D. while working full time. Your intelligence, knowledge, insights, and passion for toxicology served as a constant source of inspiration. My time at the Nassau County Medical Examiner's Office laid the foundation for the toxicologist I have become, and has ultimately set me on the path to this doctoral work. Working while under your leadership has truly been some of the most formative years of my career, and your support and encouragement gave me the tools I needed to build a strong reputation as a forensic toxicologist. I am genuinely honored that you agreed to serve on my committee, and have benefited greatly from your continued guidance. A big thanks as well to my colleagues at the Nassau County Medical Examiner's Office for all of your wisdom, kindness, and laughter over the years.

I offer sincere gratitude to Drs. Wurpel, Billack, Schanne, and Yoganathan for graciously agreeing to serve on my committee. I have learned and benefited so much from all of you, from offering guidance on how improve my research to navigating complex university administrative practices. Your insights have been invaluable throughout this process and have instilled crucial knowledge without which this research could not have been completed. I also give my thanks to the St. John's University Department of Pharmaceutical Sciences for providing their support for this research. A special thanks goes out to Dr. Reznik and her collaborators from the Montefiore Medical Center for helping move this work forward by

generously providing numerous anonymously donated human lung tissue specimens; a significant portion of this thesis would not have been possible without this assistance.

I owe immense thanks to our collaborators from the Mount Sinai Morningside Hospital, specifically Drs. Turino and Ma. Thank you for contributing your time and expertise in COPD and in the analytical chemistry of desmosine. I could never repay all the time, feedback and criticism, advice, expertise, ideas and knowledge you both so generously imparted despite your own busy schedules. I have learnt so much from both of you, and am immeasurably appreciative of all you have done.

I want to give special thanks to my lab mate, George Gu. Even though you were just about to graduate when I started, you still took time out of your schedule on multiple occasions to show me bench lab techniques I wasn't entirely familiar with, with navigating science supply during the early days of my Ph.D., and made days of misery in the lab seem fun. I also can't thank you enough for allowing me to use the tissues generated from your own thesis research in order to help advance this work.

To my dear friends Christie and Maya, I have spent years contemplating what I would write here, how ironic that I now find myself at a loss for words. The extent of your kindness and the size of your hearts have never failed to amaze me. Both of you have always been there as my biggest cheerleaders, a shoulder to cry on, the friends and confidants on whom I could always rely, and the people who always just...understood. I am incredibly fortunate to count you as my closest friends. I echo from a time early in our

friendship: Thanks. Really, just thanks. You have helped me keep the faith in the sunlit uplands when I needed it most.

Mom, Dad, and my little sister Madison: as my family, you far surpass anyone's wildest dreams. You were always there with a friendly voice and a kindly word of sympathy, advice or joy, and always ready to twist yourselves into pretzels to help me in every way imaginable. It is because of your love that I am who I am today, and your unfailing support was indispensable in realizing this accomplishment. I would also like to thank my grandmother, Omaira Buriel (1941-2012). You taught me a lot about life, though unfortunately you did not live long enough to see me finish my schooling and receive my Ph.D. But education was important to you and I know you would be proud, and I am proud to be your grandson. This thesis belongs to you.

To my wife, Bethany: From building a bookshelf in our first apartment to building a life together. You are my dearest blood, my Righteous One. You have had to bear most directly the burden of this work of mine for the past three years, and you endured with equanimity my uneven temper, buttressed my self-confidence when it flagged, and prodded me through my too frequent periods of indolence and ambition. Throughout this time, you were always as much a part of my success as I was. I shall always wear your colors into battle; I shall always wear your crest upon my shield. It is for a future with you that I have toiled, bled, and paid the price exacted upon me by this thesis. Hopefully, you can now enjoy the fruits (material and otherwise) of this labor. Our Labor. From here to the Crossroads: Together, We.

My deepest gratitude to you all.

M. Fagiola

TABLE OF CONTENTS

ACKNOWLEDGEMENTS.....	ii
LIST OF TABLES.....	viii
LIST OF FIGURES.....	ix
CHAPTER 1: INTRODUCTION.....	1
1.1 Chronic Obstructive Pulmonary Disease.....	1
1.2 Pathogenesis and Pathophysiology.....	5
1.3 Measurement of Relevant Biomarkers.....	10
1.4 Liquid Chromatography-Tandem Mass Spectrometry (LC-MS-MS).....	14
1.5 Hypothesis and Research Objectives.....	18
CHAPTER 2: MATERIALS AND METHODS.....	20
2.1 Chemicals and Reagents.....	20
2.2 Standard and Control Preparation.....	21
2.3 Sample Preparation.....	21
2.4 Solid Phase Extraction.....	22
2.5 LC Conditions.....	23
2.6 MS-MS Conditions.....	24
2.7 Re-analysis of Human Plasma, Urine, and Sputum Samples.....	25
2.7.1 Sample Transfer and Institutional Review Board Approval.....	25
2.8 Analysis of Hamster Lung Tissue.....	26
2.8.1 Study Design.....	26
2.8.2 Cigarette Smoke Exposure.....	26
2.8.3 Microscopic Studies.....	27
2.8.4 Hamster BALF Cell Content.....	27
2.8.5 Statistical Analysis.....	28
2.9 Analysis of Human Lung Tissue.....	28
2.9.1 Study Design.....	28
2.9.2 Microscopic Studies.....	29
2.9.3 Statistical Analysis.....	29
2.9.4 Institutional Review Board Approval.....	29
CHAPTER 3: RESULTS.....	31
3.1 Optimization Studies and Chromatography and DID and Desmosine-D ₄	31
3.2 Neat and Extracted Calibration Curve of DID.....	33
3.3 Chromatographic and Mass Spectral Separation of Desmosine and Isodesmosine.....	34
3.4 Method Validation.....	35
3.4.1 General.....	35
3.4.2 Linearity/Calibration Model.....	35
3.4.3 Limit of Detection (LOD) and Limit of Quantitation (LOQ).....	38
3.4.4 Bias and Precision.....	39
3.4.5 Ionization Suppression, Enhancement, and Extraction Recovery....	40
3.4.6 Selectivity, Specificity, Matrix Interferences, and Endogenous Interferences.....	41
3.4.7 Dilution Integrity.....	42
3.4.8 Processed Sample Stability.....	43
3.4.9 Carryover.....	44

3.5 Re-analysis of Human Plasma, Urine, and Sputum Samples.....	45
3.6 Hamster Lung Morphology.....	48
3.7 Hamster BALF Cell Content.....	49
3.8 Free Hamster Lung DID.....	50
3.9 Human Lung Morphology.....	52
3.10 Human Lung DID.....	53
CHAPTER 4: DISCUSSION.....	57
4.1 Preface.....	57
4.2 Evaluation of Current LC–MS Based Assays for Desmosine Analysis and Adoption of Non Ion–Paired Reverse–Phase High–Performance Liquid Chromatography.....	57
4.3 Free Lung Desmosine: A Potential Biomarker for Elastic Fiber Injury in Pulmonary Emphysema.....	62
4.4 Airspace Enlargement is Associated with Increased Elastin Crosslinking in Human Pulmonary Emphysema.....	65
CHAPTER 5: CONCLUSION.....	69
REFERENCES.....	72

LIST OF TABLES

Table 1. Gradient conditions.....	23
Table 2. Multiple reaction monitoring transitions of DID and desmosine-D ₄	24
Table 3. DID linearity evaluation.....	35
Table 4. DID residual plot calibrator levels.....	36
Table 5. Method performance.....	39
Table 6. Summary of ionization suppression, enhancement, and extraction recovery studies.....	40
Table 7. List of all exogenous compounds used for selectivity, specificity, matrix interferences, and exogenous compound interference studies (fortified at concentrations of 2500 ng/mL [ng/g]).....	42
Table 8. Stability of DID over a period of 10 days.....	43
Table 9. DID measurements in human plasma, urine, and sputum – Current method.....	45
Table 10. DID measurements in human plasma, urine, and sputum – Previous method.....	46
Table 11. Comparison of free DID levels in fresh and fixed hamster lung tissue.....	50
Table 12. Clinical histories associated with the human lung tissue specimens.....	53
Table 13. Comparison of free DID levels in fresh and fixed human lung tissue.....	53
Table 14. Comparison of total DID levels in fresh and fixed human lung tissue.....	53

LIST OF FIGURES

Figure 1. Venn diagram of chronic obstructive pulmonary disease (COPD).....	2
Figure 2. Left: Normal lung without air space enlargement. Right: Emphysematous lung with air space enlargement induced by tobacco smoke and extensive distension of the alveoli.....	2
Figure 3. Chemical structures of desmosine (left) and isodesmosine (right).....	10
Figure 4. Formation of crosslinks in elastin.....	11
Figure 5. Electrospray ionization source.....	15
Figure 6. Schematic of a triple quadrupole mass analyzer.....	17
Figure 7. Precursor and product ion characterization of desmosine (A) and desmosine-D ₄ (B). Both compounds were injected to the mass spectrometer separately to verify analyte presence in their respective reference material. The fragmentation patterns of desmosine-D ₄ are nearly identical to that of desmosine except for the mass shift due to the presence deuterium atoms.....	24
Figure 8. DID and desmosine-D ₄ (40 ng/g, un-extracted).....	31
Figure 9. DID and desmosine-D ₄ (40 ng/g, extracted).....	31
Figure 10. Chromatographs of DID with 5 μ M medronic acid (left) and without 5 μ M medronic acid (right) as a mobile phase additive [Top half of figure by J.J. Hsiao, O.G. Potter, T.W. Chu, Improved LC/MS Methods for the Analysis of Metal-Sensitive Analytes Using Medronic Acid as a Mobile Phase Additive, 2018, by permission of American Chemical Society].....	32
Figure 11. Chromatographs of extracted standards of desmosine (left), isodesmosine (middle), and combined desmosine/isodesmosine (right). Note the identical quantifier (major) transition ions as well as retention times.....	34
Figure 12. Plot of mean calibration values of DID (40 – 2000 ng/mL [ng/g]).....	35
Figure 13. Residual Plot Calibrator Levels of DID.....	36
Figure 14. Extracted ion chromatogram for desmosine at a) its limit of detection and b) its limit of quantification.....	38
Figure 15. The lung from an animal treated with cigarette smoke and LPS (left) has greater airspace enlargement than one from the group given LPS alone (center). A room	

air control lung (right) is shown for comparison. Original magnification for all 3 photomicrographs: 100x.....	48
Figure 16. Animals treated with smoke and LPS had a significantly increased MLI compared to those given LPS alone and room air controls. Numbers below bars indicate N. T-bars denote SEM.....	48
Figure 17. Animals treated with cigarette smoke and LPS showed a significant increase in total BALF leukocytes compared to room air controls. Numbers below bars indicate N. T-bars denote SEM.....	49
Figure 18. Animals treated with cigarette smoke and LPS showed a significant increase in percent BALF neutrophils compared to those given LPS alone and room air controls. Numbers below bars indicate N. T-bars denote SEM.....	49
Figure 19. Animals treated with cigarette smoke and LPS showed a significant increase in free lung DID compared to both the LPS only and room air control groups. Results include both formalin-fixed and fresh lung tissues. Numbers below bars indicate N. T-bars denote SEM.....	50
Figure 20. There was a significant positive correlation between MLI and free lung DID in both formalin-fixed and fresh lungs ($p < 0.0001$). MLI values are the means from Figure 16. Numbers in parentheses indicate N. T-bars denote SEM.....	51
Figure 21. (Left to Right) Photomicrographs of specimens showing moderate, mild to moderate, and no pulmonary emphysema. The one with moderate airspace enlargement had dilated alveolar walls with focal areas of rupture (arrows). Original magnification for all 3 photomicrographs: 40x.....	52
Figure 22. The lung tissues with moderate emphysema had a significantly greater MLI than the one with mild to moderate disease, but there was no significant difference between the two with moderate airspace enlargement. Numbers above bars indicate N. T-bars denote SEM.....	52
Figure 23. (Upper) The nonlinear regression curve indicates that accelerated elastin breakdown is associated with an MLI above 400 μm . (Lower) The level of free DID was significantly increased in tissues with moderate emphysema compared to all other groups. Numbers above bars indicate N. T-bars denote SEM.....	54
Figure 24. (Upper) A progressive increase in DID density was associated with the continued development of pulmonary emphysema. Numbers above bars indicate N. T-bars denote SEM. (Lower) A nonlinear curve (plateau followed by one phase association) more closely fit the data and was used to model the proposed relationship between DID density and MLI.....	55

CHAPTER 1:

INTRODUCTION

1.1 Chronic Obstructive Pulmonary Disease

Chronic Obstructive Pulmonary Disease (COPD) is an obstructive lung disease characterized by long-term breathing problems as a result of poor airflow, and has been used previously to describe a number of chronic lung diseases including chronic bronchitis and pulmonary emphysema (Figure 1). Chronic bronchitis has been defined as a chronic cough, with the British Medical Research Council formally defining it as a “daily productive cough for at least three consecutive months for more than two successive years” (1). Conversely, pulmonary emphysema was formally defined in 1962 by the American Thoracic Society as an “anatomic alteration of the lung characterized by an abnormal enlargement of the air spaces distal to the terminal, non-respiratory bronchiole, accompanied by destructive changes of the alveolar walls” (2).

Modifications to these definitions have been proposed due to common, as well as unique, pathophysiologic features shared by both iterations of COPD. For example, at least one investigator has stated that a diagnosis of emphysema in of itself is incomplete without a concurrent diagnosis of chronic bronchitis, and vice versa (3). Additionally, others have suggested that airspace enlargement without obvious fibrosis – a feature most commonly observed in pulmonary emphysema – is merely a structural biomarker that results secondarily to airway inflammation and destruction (4). Airspace enlargement leads to a reduction in the alveolar surface area, preventing adequate transfer of oxygen and carbon dioxide within the gas exchange regions of the lung (Figure 2). Thus, in an effort to create a more centralized and universal definition of COPD, it can be said that it

shares both airway (central and small airways) and airspace abnormalities, as opposed to strictly defining COPD as either chronic bronchitis or pulmonary emphysema alone. Because we now understand that COPD has a more complex pathogenesis, more objective measures of lung function are needed to arrive at a proper diagnosis. The analytical measurement and quantification of specific biomarkers in biological matrices can help with ascertaining structural changes that may be more inflammatory or emphysematous in nature.

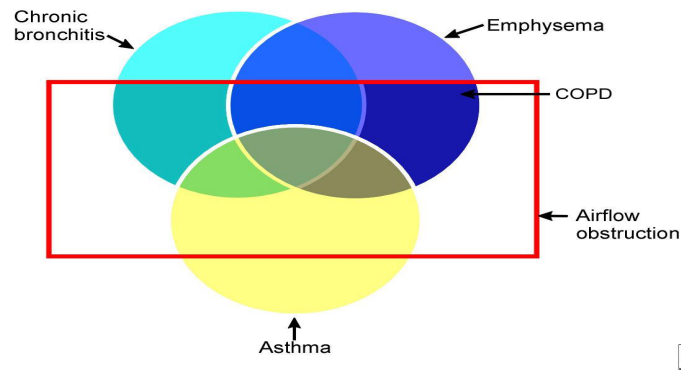


Figure 1. Venn diagram of chronic obstructive pulmonary disease (COPD).

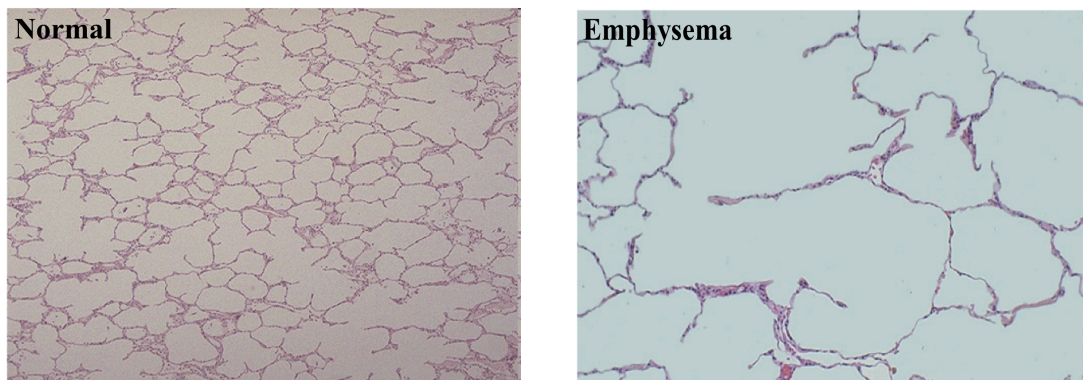


Figure 2. Left: Normal lung without air space enlargement. Right: Emphysematous lung with air space enlargement induced by tobacco smoke and extensive distension of the alveoli.

There are a multitude of risk factors that can lead to the development of COPD and are both genetic and environmental in nature. In terms of genetic factors, an established cause of COPD may result due to a considerable proteinase-antiproteinase imbalance. Alpha-1-antitrypsin deficiency (AATD) is one such genetic disease in particular that can occur in 1 to 2% of individuals with COPD (5). Alpha-1-antitrypsin is a protease inhibitor produced in the liver that is primarily responsible for protecting cells from inflammatory enzymes such as neutrophil elastase. In COPD research, studies have brought to light the role of alpha-1-antitrypsin, elastin, and the significance of AATD. Those who are homozygous for AATD are the most prone to elastin breakdown due to the decreased inhibition of elastase activity.

Further research in the genetic basis of COPD, that does not include AATD, has also lead to the identification of several loci associated with COPD susceptibility. Some of these include *CHRNA3*, *CHRNA5*, and *IREB2*, which are a series of genes responsible for nicotine dependence phenotypes in addition to the regulation of iron homeostasis under conditions of iron depletion. Additionally, genome-wide association (GWA) has been utilized to assess for mutations in various genetic sequences that give rise to the development of normal pulmonary function. Quantitatively, pulmonary function is often measured as a forced expiratory volume (FEV) and forced vital capacity (FVC). As one example, correlating an FEV-to-FVC ratio with various loci associated with pulmonary function has resulted in the identification of previously unrecognized mutated genetic sequences, such as on chromosome 13q14.3 containing a mutated *DLEU7* gene that is strongly associated with FEV decline (6). This work may ultimately

help explain other genetic etiologies and risk factors of COPD that aren't solely associated with AATD.

Tobacco smoking continues to be the primary risk factor for developing COPD. In particular, the population-attributable fraction for smoking as a cause for COPD has ranged from 9.7% to 97.9% (7). Approximately 20% of smokers will develop COPD, while this fraction increases to 50% in lifelong smokers (8). In the United States and the United Kingdom alone, 80-95% of those with COPD have been current or previous smokers (8). Additionally, women are more susceptible to the harmful effects of tobacco smoke than men (9), and second-hand smoke is attributed to approximately 20% of COPD cases in non-smokers (who may have previously smoked, but no longer do so) and never-smokers. Further, the inhalation of non-cigarette combustion products (e.g. marijuana, cigars, pipes, etc.) also confers a significant risk to the development of COPD (9).

Occupational exposure such as outdoor and indoor air pollution, dust and fumes, biomass and smoke inhalation, and exposure to second hand smoke are other risk factors that may be significant. Outdoor air pollution is mainly attributed to the emission of pollutants from motor vehicles and industrial processes. For those living in higher traffic-density areas, there is a significant association with decreased FEV and FVC, especially in women. Other particulate pollutants that may influence the development of COPD or exacerbate existing COPD include nitrogen dioxide and ozone, where increased atmospheric concentrations have also been associated with increased bronchial hyper-reactivity, airway oxidative stress, and pulmonary and systemic inflammation. Indoor air pollution includes tobacco smoke, particulate matter, carbon monoxide, biological

allergens, and many similar pollutants more often thought of as “outdoor” air pollutants including nitrogen dioxide. Among the aforementioned, tobacco smoke poses the greatest risk, though the burning of biomass (e.g. stove-top cooking) and fuel combustion associated with common kitchen appliances may substantially increase the risk of COPD (9). A recent meta-analysis based on 15 epidemiologic studies concluded that biomass smoke exposure was a significant risk factor for developing COPD in both men and women, with the strongest associations seen in current and former cigarette smokers regardless of gender (10).

1.2 Pathogenesis and Pathophysiology

The pathological changes associated with inflammatory and emphysematous COPD has been well documented. Both histological and pathological changes can be observed in the central airways, the small airways, and the alveolar space during active disease (11). For example, mucus glands and goblet cells are enlarged and undergo metaplasia in the COPD patient, whereas these are normally defined in the lining of the trachea and the bronchi in healthy patients. Additionally, the combined enlargement of mucus glands and goblet cells results in an increased secretion of mucus itself. Taken together with the irritating nature of cigarette smoke and resultant immotility of cilia within the trachea-bronchial tree, the efficacy of mucociliary clearance is ultimately reduced and a chronic cough can develop due to the buildup of mucus, among other symptoms. However, there are multiple hypotheses for the proposed pathogenesis of COPD; these include a proteinase-antiproteinase imbalance as briefly described earlier, immunological mechanisms, oxidant-antioxidant balance, systemic inflammation, apoptosis, and ineffective cellular repair and regeneration (11).

The proteinase-antiproteinase imbalance phenomenon has stemmed predominantly from studies to ascertain the role of alpha-1-antitrypsin, the significance of alpha-1-antitrypsin deficiency, and greater-than-normal degradation of elastin in COPD patients, which was first reported by Laurell and Eriksson in 1963 (12). The hypothesis is based on the assumption that COPD can develop due to the imbalance of proteinases that breakdown elastic tissue and antiproteinases which effectively act as “antagonists” towards elastin-degrading enzymes like neutrophil elastase. A higher proteinase-to-antiproteinase ratio results in an increased amount of inflammatory proteinase activity as seen in COPD. With respect to AATD, mutations in the alpha-1-antitrypsin gene impair its secretion from hepatocytes that result in decreased circulating antiproteinase concentrations. Patients who are heterozygous for this mutation are still at risk for a proteinase-antiproteinase imbalance, but those who are homozygous for the mutation are at the highest risk for developing COPD. The reduced circulation of alpha-1-antitrypsin also increases the chances for developing generalized inflammation due to impaired neutrophil elastase inhibition. As mentioned earlier, cigarette smoking is one of the biggest risk factors in developing COPD, and those with AATD who are known to be chronic cigarette smokers have shown an increased accumulation of pulmonary macrophages, neutrophils, and CD8⁺ T-lymphocytes, and these immunogenic cells are some of the most common sources of inflammatory proteases in the lungs. (13) Excess neutrophil elastase as a result of the accumulation of these aforementioned cells overwhelms antiproteinase function, and will lead to the development of COPD. In addition to proteinases like neutrophil elastase and antiproteinases like alpha-1-antitrypsin, matrix metalloproteinases (MMPs – specifically MMP-9) are also linked to

the pathogenesis COPD, as they are responsible for the breakdown of collagen and elastin (14). MMP-9 has been shown to increase as a result of smoking-related COPD, in addition to increased production of MMP-9 by macrophages in direct response to the irritant nature of cigarette smoke. The inflammatory and protease burden creates a feedback loop that may lead to further destruction of the lung parenchyma by MMP-9 once COPD has developed.

Through the increased production and circulation of proteinases by macrophages and immunogenic cells, there is a concomitant abnormal inflammatory response that arises as a result of the exposure to particles, pollutants, and most commonly cigarette smoke. In an early study to correlate COPD disease states to inflammatory response, Pesci et al. found that patients with active COPD exhibited increased concentrations of neutrophils in sputum, lung tissue, and bronchoalveolar lavage fluid (BALF) (15). Braber et al. additionally found increased serum immunoglobulin free light chains (IgLC) in those suffering from smoking-induced COPD (16). Braber et al. further determined that IgLC binds neutrophils and crosslinks with other neutrophil-bound IgLCs that, in turn, results in an increased production of the neutrophil attractants IL8/CXCL8, a group of cytokines expressed by leukocytes. Additionally, it has also been reported that IgE-mediated inflammatory responses – when combined with IgLC proinflammatory effects – can exacerbate existing COPD via increased neutrophil activity, though the extent of these mechanisms are not yet fully understood (16).

The proteinase-antiproteinase imbalance hypothesis and any subsequent inflammatory mechanisms that follow this pathophysiologic state have encouraged the use of elastase inhibitors as potential treatments for COPD. However, this approach has

been met with little success, and clinical testing of various inhibitors has failed to produce successful therapeutic options for COPD (17). There has been extensive research into alternative pathophysiologic mechanisms that could explain the pathogenesis of COPD, possibly as an adjunct to the proteinase-antiproteinase imbalance hypothesis. Abnormally accumulated inflammatory cells, such as neutrophils and macrophages, as a result of cigarette smoking produce reactive oxygen species (ROS). ROS are produced from superoxide anions and can include hydroxyl radicals, singlet oxygens, and superoxides. In a biological context, ROS is a normal byproduct of natural aerobic respiration and, under normal conditions, are intrinsic to cellular function and do not have long-term pathophysiologic consequences. However, production of ROS in excess (as in cigarette smoking) can cause irreversible DNA damage, initiate lipid peroxidation, modify cellular components, and form protein adducts. It is no surprise that ROS are indicated in the pathogenesis of COPD, as oxidative stress impairs vasodilation and endothelial cell growth in the lung. When oxidant load exceeds antioxidant capacity, tissue injury occurs within the microenvironment of the lung. ROS can modify elastin, and modified elastin is more susceptible to proteolysis by elastases as well as MMPs, augmenting the matrix-degrading capacity conducive to the development of COPD (11).

Extrapulmonary inflammation has been shown to be a significant component of COPD pathogenesis, as persistent inflammation promotes the release of inflammatory cytokines, which in turn stimulate the release of leukocytes, TNF- α , and a number of other inflammatory cell types into circulation. This systemic inflammation not only exacerbates COPD, but may also worsen other health conditions. Two population studies involved nearly nine thousand COPD patients and revealed that elevated levels of

inflammatory cells increased the risk of major comorbidities – including myocardial infarction, lung cancer, and pneumonia – often seen in those with COPD (18).

Finally, other mechanisms of COPD pathogenesis include aspects of apoptosis, ineffective lung cell repair, and the formation of endothelial microparticles in COPD-associated vascular disease. Increased apoptosis has been demonstrated in COPD patients, particularly in the alveolar epithelial and endothelial cells in the lungs of COPD patients. Unlike proteinases/antiproteinases or oxidants/antioxidants, there is no counterbalance to increased COPD-mediated increases in apoptosis, with the net result of the destruction of lung tissue and the development and possible exacerbation of COPD. This is compounded by ineffective cellular repair in the lungs of COPD patients due to extensive damage of alveolar cells within the gas exchange region. The development of endothelial microparticles (a hallmark of vascular disease) is another known comorbidity of COPD, and can contribute to COPD symptoms including pulmonary hypertension. Endothelial microparticles are complex vesicular structures shed from activated or apoptotic endothelial cells and are increased in those who smoke, and may be a potential biomarker of vascular diseases associated with COPD (19). They additionally play a significant role in coagulation, inflammation, endothelial function, and angiogenesis and thus disturb vascular homeostasis, contributing to the progression of vascular diseases (19).

1.3 Measurement of Relevant Biomarkers

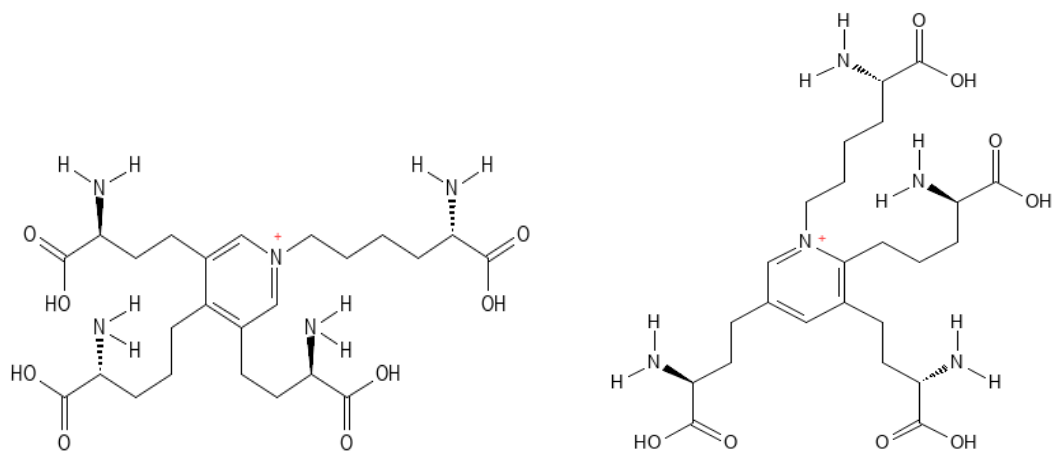


Figure 3. Chemical structures of desmosine (left) and isodesmosine (right).

In the assessment of the clinical presentation and response to therapy in COPD, there has long been a major need for the identification of suitable and reproducible physiologic parameters and biochemical indicators (Figure 3) in order to evaluate disease progression and changes during therapeutic intervention (20). This has been somewhat met by the previously mentioned, albeit less sensitive, parameters including FEV₁, FVC, and other diagnostic tests such as computed tomography. Unfortunately, these are limited in that they provide only a measure of the pathophysiologic consequences of COPD (e.g. reduced capacity), but are not *biomarkers* as traditionally defined, nor are they considered to be an adequate surrogate end-point for the progression of disease. The United States National Institutes of Health (NIH) defines a biomarker as “a characteristic that is objectively measured and evaluated as an indicator of normal biological processes, pathogenic processes, or pharmacological responses to therapeutic intervention” and more simply can be considered a direct indicator of the processes being studied (21).

Moreover, these biomarkers might typically refer to a molecule, endogenous or exogenous, and may be pathogenic in nature.

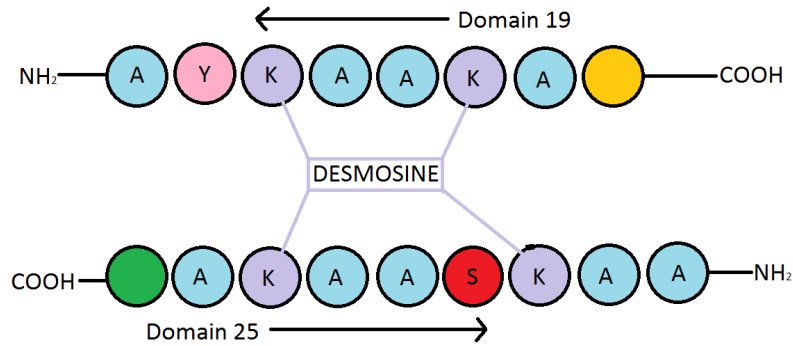


Figure 4. Formation of crosslinks in elastin.

In the search for biomarkers unique to the pathogenesis and progression of disease in COPD, desmosine (DID) is one such molecule that stands out. Desmosine (D) is a unique amino acid found uniquely in elastic arteries and – along with its isomer isodesmosine (ID) – gives rise to elasticity in this tissue via crosslinking in a reaction catalyzed by lysyl oxidase (Figure 4). This is especially important for elastin in the lung, as DID is responsible for providing the elasticity necessary for the organ to perform the normal breathing cycle. In cases where elastin is broken down like in COPD, or where turnover is increased substantially such as in cases of COPD brought on by AATD, DID can be measured through analytical means as an indicator of this pathophysiological process. Because DID is unique only to mature elastin, it has been useful in discriminating elastin breakdown-derived peptides from precursor elastin peptides. DID has also been extensively evaluated as an indicator of the effectiveness of agents with the

potential to reduce elastin breakdown. Both Cantor et al. (17) and Ma et al. (22) have recently demonstrated it was possible to show a decrease of DID in plasma, urine, and sputum from patients with diagnosed COPD following the administration of tiotropium and aerosolized hyaluronan, respectively, lending more promise of classifying DID as a novel biomarker of COPD.

DID is one of the oldest COPD biomarker candidates, having been introduced in the early 1960s (23) and the detection and measurement of DID as a means of study of elastin degradation has been recognized in past years. Some of the earliest methodologies were based on immunological techniques including radioimmunoassay as a means of measuring DID via urinary excretion, which preceded the development of an ELISA for the measurements of DID in plasma and urine (24). Since its inception as a potential biomarker in COPD, there has been an abundance of data with respect to methods of detection and measurement, including further refinement of existing analytical methods utilizing isotope dilution to increase quantitative accuracy of DID measurements. However, DID has not yet been considered to be a valid biomarker in the assessment of a slowly progressive disease such as COPD to date. Acceptance of DID as a biomarker of COPD is limited by methodologic concerns related to accurate quantification despite recent analytical improvements. Inconsistency of quantitative results and poorly validated methods (each of which may have been developed under different method validation guidelines) are some of the major reasons for its lack of acceptance. Additionally, there have been no attempts to measure DID directly in lung tissue, with methods so far only focusing on urine, plasma, sputum, and bronchoalveolar lavage (BALF), which are considered to be ‘per se’ indicators of elastin breakdown. Interpretation of DID

concentrations in the aforementioned matrices is complicated in that, aside from BALF and sputum, DID measurements are not specific to COPD in the lung, but instead may be attributed to elastin breakdown in other diseases and from other organs where elastin turnover is also increased (e.g. heart disease and atherosclerosis). Such extraneous factors may contribute to varying levels of DID in patients with a similar clinical progression or stage of disease whereas the ultimate objective is to measure the degradation of mature elastin *in situ* and not include precursor elastin molecules or other sources that could confound the analysis. Further analytical problems can be traced to issues of sensitivity and accurate quantitation of DID in BALF and sputum due to low rates of excretion in these matrices.

Furthermore, while DID can satisfy certain biomarker criteria including being central to the pathophysiologic process, being a “true” surrogate end-point in disease progression, and with varying concentrations with respect to disease progression, it still falls short. It still has not been shown that DID concentrations correlate directly to the severity of disease (due, in part, to a lack of data of DID measurements in the lungs of patients with COPD), it has not been able to predict disease progression, and it must reflect changes induced by effective therapeutic treatments. Liquid chromatography-tandem mass spectrometry (LC-MS-MS) has been extensively utilized in recent years in the quest to further define DID as a valid biomarker in COPD.

1.4 Liquid Chromatography-Tandem Mass Spectrometry (LC-MS-MS)

Following its development in the early 20th century, mass spectrometry has been applied in a wide variety of scientific disciplines. Advancements in the technology have lead to the large-scale production of smaller, more efficient, and relatively inexpensive instruments (25). In particular, liquid chromatography-tandem mass spectrometry (LC-MS-MS) has gained wider favor for the analysis of DID over more conventional mass spectrometry techniques including single quadrupole gas chromatography-mass spectrometry (GC-MS) and single quadrupole liquid chromatography-mass spectrometry (LC-MS). LC-MS-MS is a powerful tool in quantitative and targeted tandem mass spectrometry experiments, especially for the analysis of product ions for structure elucidation. The full extent of its capabilities are fully realized when the user has background knowledge with respect to the behavior and analytical chemistry of the target analyte(s). There is a significant learning curve for this type of instrument, and good signal-to-noise (S/N), selectivity, specificity, and decreased interferences may require prior knowledge of the chromatographic and mass spectral characteristics of the target analyte. The proper chromatographic and mass spectral characterization of a target analyte on LC-MS-MS may also involve an extensive method development and validation process, depending on the standards adhered to.

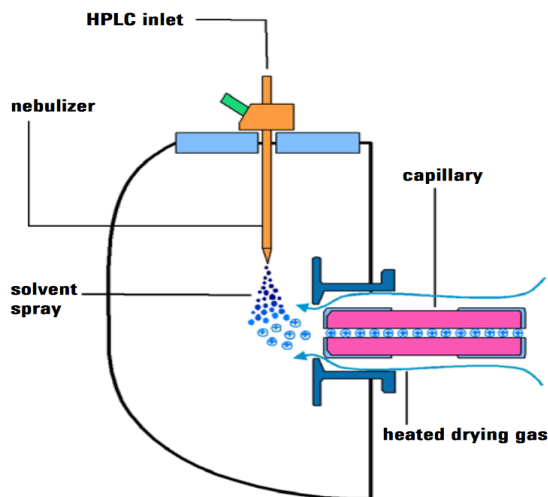


Figure 5. Electrospray ionization source

Prior to conducting mass spectral analysis of any analyte or analytes, they must first be fragmented into ions. This process is important because the analyte must be a charged species in order to be detected. DID at its pyridinium ring or any of its carboxylate functional groups may already be charged at physiologic pH, thus requiring the need for the adjustment of chromatograph mobile phase pH to optimize DID retention. This facilitates better chromatographic separation for the most optimal S/N. Once chromatographically separated, the analyte is introduced to an electrospray ionization (ESI) source, a form of soft ionization used to produce gas phase ions and does not result in significant fragmentation.

An ESI source in a typical LC–MS-MS system is shown in Figure 5 (26). Inside the ESI source, ionization occurs in three steps: 1) dispersal of a mist composed of charged droplets, 2) evaporation of the solvent, and 3) ejection of the ion from the highly charged droplets. The sample solution introduced from the LC portion of the system is delivered to a capillary, which is then nebulized and dispersed as a mist by nitrogen and a

voltage is applied. The mobile phase solvent continues to evaporate and decrease in size in the source until the charge exceeds the surface tension of the droplet (known as the rayleigh limit). When the electric field strength reaches a critical point, the ions at the surface of the droplets are ejected into the gaseous phase in a process known as coulombic dissociation, leaving only a stream of charged ions that are attracted to the source capillary and subsequently the first quadrupole analyzer by an electric potential gradient. Depending on the physicochemical properties of the analyte, it may be positively or negatively charged following introduction to the source. Acids tend to be ionized in “negative” ESI, while bases are often ionized in “positive” ESI.

DID is unique in that it is an amphoteric compound and therefore exhibits both acidic and basic characteristics. Interestingly, DID is often extracted from biological matrices utilizing cation exchange solid phase extraction techniques that are optimized for weak bases. In addition, DID can be successfully analyzed in positive ESI, but through the production of an $[M]^+$ molecular ion as opposed to $[M+H]^+$ molecular ions often produced in positive ESI or $[M-H]^-$ molecular ions often produced in negative ESI. This is due, in part, to the charged nature of the pyridinium ring present in DID's structure that would otherwise form an unstable radical cation through $[M+H]^+$ production.

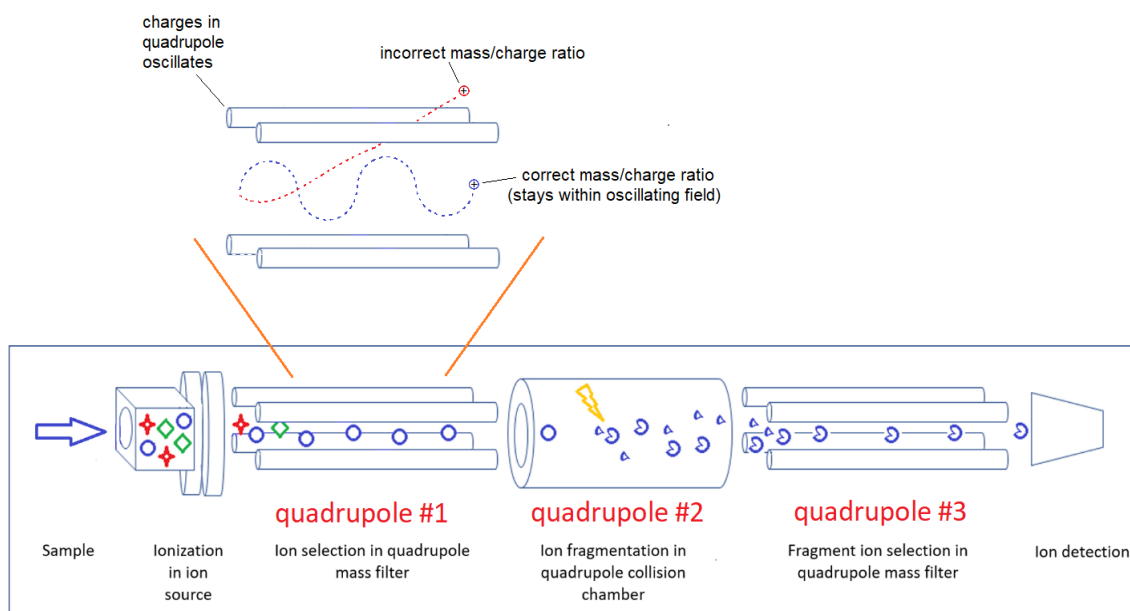


Figure 6. Schematic of a triple quadrupole mass analyzer

The basic hardware of a triple quadrupole LC–MS-MS system operating in multiple reaction monitoring [MRM] mode is described in Figure 6. Briefly, a mass (or multiple masses) selected precursor(s) ion(s) is/are chosen with the first quadrupole (quadrupole #1). The collision cell (quadrupole #2) then generates fragment ions. The second quadrupole (quadrupole #3) is programmed to look for those specific fragment ions (quantifier and qualifier product ions) produced from the collision cell. This form of targeted mass analysis provides many advantages for the quantitative analysis of DID and other analytes. In single quadrupole systems, the m/z ratio acquired may not always be sufficient to confirm the presence, or absence, of an analyte, as illustrated by the existence of potential structural isomers of such analytes (27). Though it may be possible to distinguish such analytes by adjusting the chromatographic separation, there is no guarantee of achieving baseline separation. With the advent of triple quadrupole LC–MS-MS, one can make use of two quadrupole analyzers with a collision cell. The production

of unique transition ions in the collision cell reduces the possibility of interferences and misidentification of the target analyte, owing to the isolation of the precursor ion in the first quadrupole and determination of the presence of the unique transition ions related only to that single precursor (27).

1.5 Hypothesis and Research Objectives

We hypothesize that DID is a potential biomarker for emphysematous changes in COPD. Additionally, we hypothesize that increases in DID in biological fluids correlate with the degree of pulmonary airspace enlargement, that the level of peptide-free DID in lung tissue is a sensitive and specific marker for pulmonary emphysema, and that the density of DID in lung tissue may vary with mechanical strain imposed by airspace enlargement.

Because there have been no attempts to measure DID in both fresh lung tissue and formalin-fixed, paraffin-embedded human lung tissue (FFPE), the following objectives were proposed for this research:

- 1.** To develop and validate an LC–MS-MS method for the quantification of DID in fresh and FFPE human lung tissue. This has not been previously attempted and is novel to the current study.
- 2.** While it is critically important for this research that an appropriate LC–MS-MS method is developed to measure DID in human lung tissue, the need for quantifying DID in other matrices is still apparent. This is important when correlating DID concentrations in multiple matrices with the efficacy of potential therapeutic treatments, wherein DID may be utilized as a “decision-point” for further clinical trial development of COPD drugs, and as a surrogate end-point for disease progression. Thus the LC–MS-MS method

should also be able to simultaneously analyze DID in urine, plasma, sputum, and BALF in addition to human lung tissue. Current LC–MS-MS methods for DID have not attempted to analyze different biological matrices simultaneously.

3. Though fluids such as urine, plasma, sputum, and BALF may act as ‘per se’ indicators of elastin breakdown in the lung, the advantages and objective of analyzing DID both simultaneously in human lung tissue and fluids includes the ability to correlate biochemical changes with localized tissue morphology.

4. The morphological-biochemical correlations derived from this study would provide significant insight into the relationship between the loss of elastin and airspace enlargement as a direct relationship with DID concentration.

5. To additionally establish DID as a diagnostic tool for forensic pathologists in the pursuit of establishing the cause and manner of death where no apparent airway injury is present during autopsy.

6. Finally, positive findings would support the hypothesis that elastin degradation plays an important role in the pathogenesis of COPD. Effectively constructing a morphological-biochemical topological map of the lung would offer previously unavailable insights into the biochemical changes responsible for the topological spread of emphysematous changes and the pattern of progression of COPD throughout the lung.

CHAPTER 2: MATERIALS AND METHODS

2.1 Chemicals and Reagents

A commercial reference standard of desmosine to prepare the calibrator working solution was purchased from Elastin Products Company (Owensville, MO, USA) at a mass of 5.0 mg and prepared at a concentration of 1.0 mg/mL in water. A commercial reference standard of desmosine chloride to prepare the quality control (QC) working solution was purchased from Toronto Research Chemicals (North York, ON, CA) at a mass of 1.0 mg and prepared at a concentration of 1.0 mg/mL in water. An isotopically labeled desmosine-D₄ reference standard was also purchased from Toronto Research Chemicals at a mass of 1.0 mg and prepared at a concentration of 1.0 mg/mL in water.

Formic acid, ammonium formate, and xylene were acquired from VWR Chemicals (Radnor, PA, USA) and Sigma-Aldrich (St. Louis, MO, USA). ACS and LC-MS grade methanol were acquired from VWR Chemicals and Fisher Scientific (Waltham, MA, USA). ACS grade hydrochloric acid and ammonium hydroxide were purchased from VWR Chemicals. Medronic acid (purchased as the InfinityLab[®] Deactivator Additive) was purchased from Agilent Technologies (Santa Clara, CA, USA). Ultrapure water (>18.0 MΩ-cm resistivity) was acquired in-house using a Milli-Q IQ 7005 Water Purification System from Millipore Sigma (Burlington, MA, USA). All solvents employed are LC-MS grade or higher in the chromatographic system.

2.2 Standard and Control Preparation

DID calibrator and QC working solutions were prepared in methanol from the purchased reference standards at concentrations of 4.0 µg/mL each. A desmosine-D₄ internal standard working solution was also prepared in methanol at a concentration of 10.0 µg/mL. All working solutions were stored in amber vials at <0°C when not in use. Individual calibrator samples were prepared by fortifying solid tissue specimens prepared from sheep brain homogenate (Carolina Biological Supply Company, Burlington, NC, USA) at concentrations of 40, 100, 500, 1000, and 2000 ng/mL (ng/g). Three positive QC specimens with target concentrations of 150, 400, and 800 ng/mL (ng/g) in donor plasma (UTAK Laboratories Inc., Valencia, CA, USA), donor urine (UTAK Laboratories Inc.), and tissue respectively as well as a negative tissue QC sample containing only the internal standard were analyzed to verify the calibration. A high control sample containing 2500 ng/mL (ng/g) of desmosine was analyzed to assess for carryover.

2.3 Sample Preparation

Sheep brain was selected as the matrix of choice to prepare the calibration curve. Brain is comprised of predominantly fatty tissue with a quantitatively negligible amount of elastin and serves to account for potential matrix effects encountered in solid tissue specimens while also eliminating the concern of endogenous desmosine potentially contributing to the detector signal. 5 g of sheep brain was weighed and added to 50 mL plastic centrifuge tubes containing 20 mL of ultrapure water. This mixture was then mechanically homogenized by a Brinkmann Polytron Homogenizer PT 10/35 (Westbury, NY, USA). If total DID (nonpeptide-bound + peptide-bound) was analyzed, the resulting homogenate was hydrolyzed in 6 N HCl for 24 hours at 100°C, while no hydrolysis step

was needed if free DID was analyzed. The homogenized samples then underwent centrifugation for 20 min at 3000 rpm. 1 mL of the resultant supernatant was then aliquoted into 15 mL plastic centrifuge tubes and fortified with the internal standard, calibrator, and QC working solutions as described above. Authentic hamster and human wet lung tissue specimens were processed in the same manner as the calibrator and QC samples to measure either free or total DID and fortified only with the internal standard. 1 mL of human plasma, urine, and sputum samples were aliquoted directly and fortified with the internal standard. In wet lung, units of ng/g were used.

FFPE human lung tissue slides were processed prior to the described SPE procedure in order to remove the paraffin wax prior to LC-MS-MS analysis. The slides were placed upright in a rack and heated for 15 min in a preheated oven at 110°C. After heating, the liquid paraffin was drained off and followed by a 100% xylene wash step for 10 min with occasional mild stirring. The slide was then allowed to fully dry. The deparaffinized lung tissue was carefully scraped off the glass slides and weighed. Finally, the lung tissue was hydrolyzed in 6 N HCl for 24 hours at 100°C prior to SPE for analysis of total DID in units of ng DID per mg lung tissue.

2.4 Solid Phase Extraction

DID and desmosine-D₄ were extracted from the aforementioned biological matrices by cationic exchange solid phase extraction (SPE) utilizing Styre Screen[®] BCX Extraction Columns (United Chemical Technologies Inc., Bristol, PA, USA). The cation exchange sorbent serves to retain DID and desmosine-D₄. First, 3 mL of 0.1 N HCl (pH ~ 1.0) was added to 1 mL of fortified calibrator/QC and authentic/unknown samples, followed by a quick vortex and centrifugation for 10 min at 3000 rpm prior to column

loading. The SPE cartridges were conditioned with 4 mL of methanol followed by 3 mL of 0.1 N HCl. Subsequently, the samples (3 mL of the pre-added 0.1 N HCl and 1 mL of plasma, urine, or tissue homogenate containing DID and desmosine-D₄) were loaded into each designated pre-conditioned column and were allowed to drip with gravity flow. A series of wash steps were performed on each column in the order of 3 mL of 0.1 N HCl and 4 mL of methanol. The columns were then allowed to dry at full vacuum for 30 seconds. Elution of DID and desmosine-D₄ was utilized with 3 mL of a solvent prepared fresh as a mixture of 95% methanol and 5% concentrated ammonium hydroxide. Eluents were evaporated to dryness under vacuum using a rotovap, and the residues were reconstituted in 200 µL of a 95:5 mixture of ultrapure water and methanol and injected into the chromatographic system.

2.5 LC Conditions

Table 1. Gradient Conditions

	Time (min)	Mobile Phase A – Aqueous (%)	Mobile Phase B – Organic (%)
1	0.00	95%	5%
2	3.00	95%	5%

An Agilent 1260 LC equipped with a Poroshell 120 EC-C18 column (3.0 mm x 50 mm, 2.7 µm) was utilized for the chromatographic separation of DID and desmosine-D₄. The LC column was maintained at 50°C in the thermostated column compartment. Mobile phases consisted of (A) 0.01% formic acid, 5mM ammonium formate, and 5 µM medronic acid in ultrapure water (Millipore Sigma) and (B) 0.01% formic acid and 5 µM medronic acid in LC-MS grade methanol. The mobile phase flow rate was 0.25 mL/min and the instrument injection volume was 2.5 µL. The total chromatographic run time was 3 min (Table 1), with a post-time of 3 min.

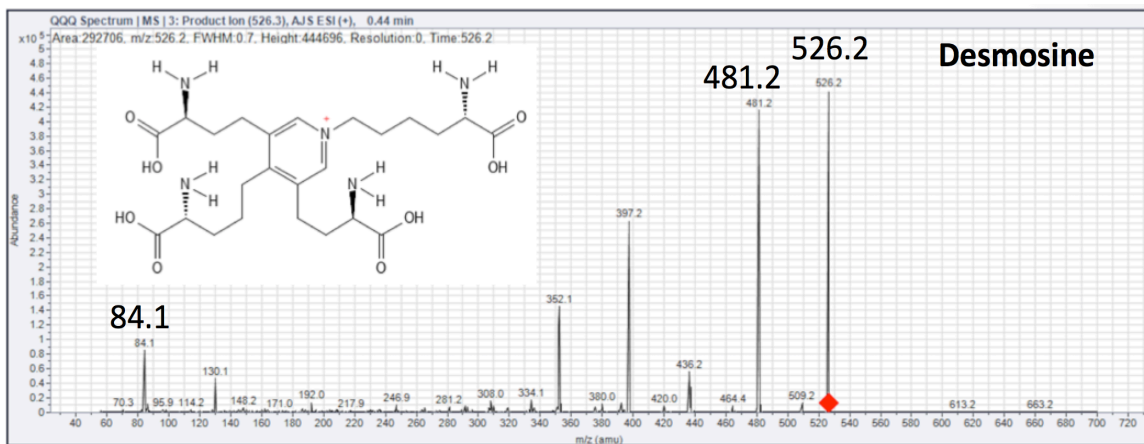
2.6 MS-MS Conditions

Table 2. Multiple reaction monitoring transitions of DID and desmosine-D₄

Analyte name	Precursor ion (<i>m/z</i>)	RT (min)	Fragmentor (V)	Product ion 1 (<i>m/z</i>)	CE 1 (V)	Product ion 2 (<i>m/z</i>)	CE 2 (V)
Desmosine-D ₄	530.3	1.359	171	485.2	36	N/A	N/A
Desmosine (DID)	526.3	1.360	176	481.2	36	84.1	55

m/z, mass-to-charge ratio; RT, retention time; V, voltage; CE, collision energy; N/A, not applicable.

A. Desmosine



B. Desmosine-D₄

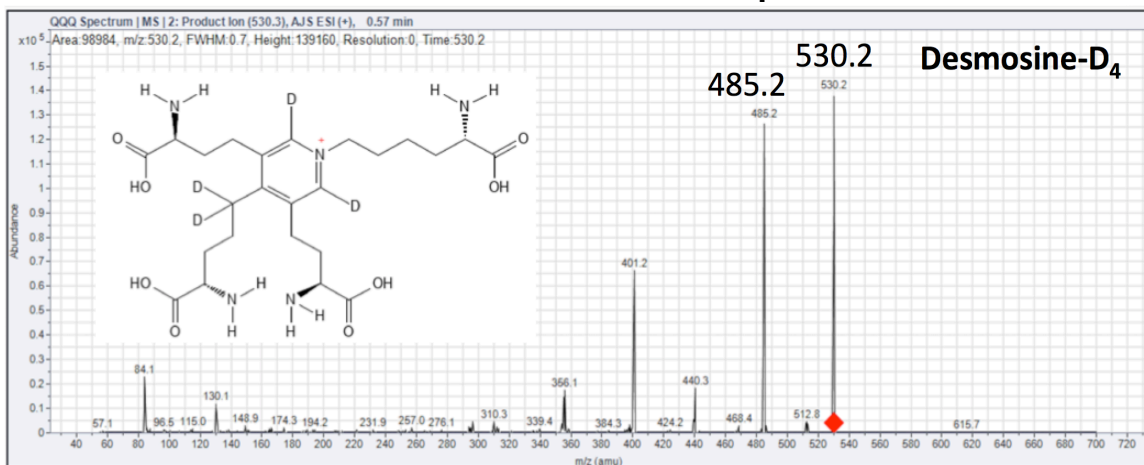


Figure 7. Precursor and product ion characterization of desmosine (A) and desmosine-D₄ (B). Both compounds were injected to the mass spectrometer separately to verify analyte presence in their respective reference material. The fragmentation patterns of desmosine-D₄ are nearly identical to that of desmosine except for the mass shift due to the presence deuterium atoms.

An Agilent Technologies 6460-triple quadrupole mass spectrometer with a dual jetstream electrospray source was operated in positive ion mode with the following parameters: drying gas temperature 325°C, nitrogen sheath gas temperature 390°C, nitrogen drying gas flow 13 L/min, nitrogen sheath gas flow 12 L/min, nebulizer pressure 35 psi, and capillary voltage 3750 V. The MRM method monitored two transitions for DID and one transition for desmosine-D₄ (Table 2). For DID, one MRM transition served as a quantifier transition and the second MRM transition served as a qualifier transition. All analyte-specific parameters were optimized using individual reference standards and analyzed in product ion mode to verify analyte presence (Figure 7). All MRM transitions utilized in the method are diagnostic of the target compounds.

2.7 Re-Analysis of Human Plasma, Urine, and Sputum Samples

2.7.1 Sample Transfer and Institutional Review Board Approval

Human bodily fluid samples which included plasma, urine, and sputum were obtained following the completion of a phase 2, multicenter, randomized, double-blind, parallel-group, placebo-controlled, proof of concept study in subjects with pulmonary emphysema secondary to alpha-1-antiprotease deficiency. The protocol and informed consent documents for the previous study as well as for their transfer and reanalysis for the purposes of this study were reviewed and approved by an institutional review board (IRB) at each participating site under protocol IRB-FY2021-255.

2.8 Analysis of Hamster Lung Tissue

2.8.1 Study Design

The study was designed to evaluate both formalin-fixed and unfixed lung tissue for free DID in hamsters treated with either cigarette smoke and LPS, room air and LPS, or room air alone. Female golden Syrian hamsters (Envigo, Somerset, NJ), weighing between 90-100 grams were exposed to either secondhand cigarette smoke for 4 hours per day over a period of 3 days or room air. 24 hours later, animals from both groups were injected intraperitoneally with either 200 µg LPS in 0.1 mL saline or saline alone. On the following day, animals were euthanized via carbon dioxide (CO₂) asphyxiation and subjected to bronchoalveolar lavage prior to measurement of free DID. Additional lungs were inflated with neutral-buffered formalin for microscopic examination or DID analysis. A total of 56 animals were used in the study and each measurement involved a minimum of 3 replicates. All experimental procedures were reviewed and approved by the Institutional Animal Care and Use Committee (IACUC) at St. John's University under protocol number 1915. Animals were housed in St. Albert Hall and all experiments were performed at the same location with timely access to veterinary assistance.

2.8.2 Cigarette Smoke Exposure

Animals (2-3 per cage) were placed inside a 28 × 19 × 15 in chamber and exposed to whole body sidestream secondhand cigarette smoke for 4 hours per day over a period of 3 days. The smoke was produced by a TE-10 smoking machine (Teague Enterprises, Davis, CA) which simultaneously burned two filtered University of Kentucky type 3R4F research-grade cigarettes (Teague Enterprises). Each cigarette was puffed once per minute for 2 seconds at a flow rate of 1.0 L/min. This process was repeated nine times

before ejecting the cigarette and loading a new one. Proper flow rate was maintained by a vacuum pump that established negative pressure at the exhaust port. The level of suspended smoke particulates within the chamber averaged 15.7 mg per mm³.

2.8.3 Microscopic Studies

Lungs were inflated *in situ* using 10% neutral-buffered formalin at a pressure of 20 cm H₂O. Both the lungs and heart were then excised as a single block and fixed in formalin for at least 48 hours. Following removal of extrapulmonary structures, the lungs were randomly cut into sections, submitted for histological processing, and stained with hematoxylin and eosin. Photomicrographs of the lung slides were taken at 100x magnification by a person unfamiliar with the design of the study and processed with ImageJ software (National Institutes of Health, Bethesda, MD) to determine airspace size using the mean linear intercept (MLI) method (28). Microscopic fields containing prominent blood vessels or airways were not included in the measurements, and areas of hyperinflation or inadequate inflation were also excluded. A standard linear test grid was applied to a minimum of 25 photomicrographs of known microscopic dimension, and the intersection of grid lines with alveolar septa were counted to determine mean airspace diameter.

2.8.4 Hamster BALF Cell Content

Following euthanasia, lungs were lavaged 3 times with normal saline, using a 5 mL syringe attached to a catheter inserted in the trachea. The samples were then centrifuged and the cell pellet was resuspended in 1 mL of normal saline for measurement of total leukocytes with a hemocytometer. Differential cell counts were performed by plating the cells onto microscope slides with a cytopsin centrifuge (Shandon Inc., Pittsburgh, USA),

and treating them with Wright-Giemsa stain. The percentage of neutrophils was determined by examining a total of 200 leukocytes.

2.8.5 Statistical Analysis

One-way analysis of variance (ANOVA) with the Bonferroni post-hoc test was used to determine if there were statistically significant differences ($p < 0.05$) among the treatment groups. Linear regression was performed to determine whether the relationship between MLI and free lung DID was significant ($p < 0.05$). All results were expressed as mean \pm standard error of mean (SEM).

2.9 Analysis of Human Lung Tissue

2.9.1 Study Design

This study had two main objectives: 1) to determine the level of free DID in formalin-fixed lung tissue from individuals with either COPD or no history of the disease and to correlate the results with airspace size, and 2) to measure total DID in FFPE tissue sections and to correlate the results with airspace size. Formalin-fixed human lung tissue was obtained from the Montefiore Medical Center Department of Pathology (Bronx, NY, USA). A fresh specimen procured from the National Disease Research Interchange (Philadelphia, PA, USA) was fixed in our laboratory prior to analysis. The clinical histories associated with the specimens are shown in Table 11. Free lung DID was determined using LC-MS-MS. Additional tissue was submitted for histological processing and either stained with hematoxylin and eosin (H&E) for morphometry or left unstained for measurement of total DID. The H&E sections were measured for airspace size, using the MLI method, and total lung surface area (13). The results were then compared with free lung DID in wet tissue and total DID in the FFPE sections to

determine whether increased elastin breakdown is associated with alveolar wall distention and to construct a map of DID density in normal and emphysematous lungs at the microscopic level.

2.9.2 Microscopic studies

The human lung tissues used in these studies were inflated with formalin at the time of fixation to ensure proper expansion of air spaces. Following removal of large airways and blood vessels, they were cut into multiple pieces and submitted for histological processing. Photomicrographs of the H&E slides were taken at 100x magnification and processed with ImageJ software to determine airspace size by using MLI (28). Microscopic fields containing prominent blood vessels or airways were not included in the measurements, and areas of hyperinflation or inadequate inflation were also excluded. A standard linear test grid was applied to a minimum of 25 photomicrographs of known microscopic dimension, and the intersection of grid lines with alveolar septa were counted to determine mean airspace diameter.

2.9.3 Statistical Analysis

One-way analysis of variance (ANOVA) with the Bonferroni post-hoc test was used to determine if there were statistically significant differences ($p < 0.05$) between diseased and healthy groups. Linear regression was performed to determine whether the relationship between MLI, total lung tissue, and free lung DID was significant ($p < 0.05$). All results were expressed as mean \pm standard error of mean (SEM).

2.9.4 Institutional Review Board Approval

The protocol and informed consent documents for this study as well as for their transfer and analysis for the purposes of this study were reviewed and approved by an

institutional review board (IRB) at each participating site under protocol IRB-FY2021-184.

CHAPTER 3: RESULTS

3.1 Optimization Studies and Chromatography of DID and Desmosine-D₄

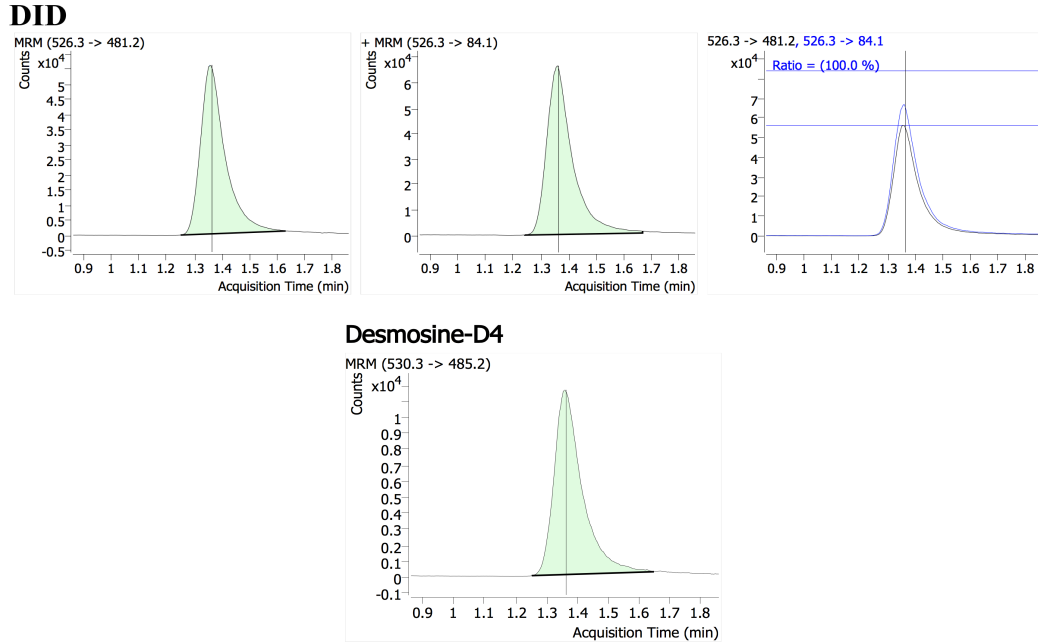


Figure 8. DID and desmosine-D₄ (40 ng/g, neat)

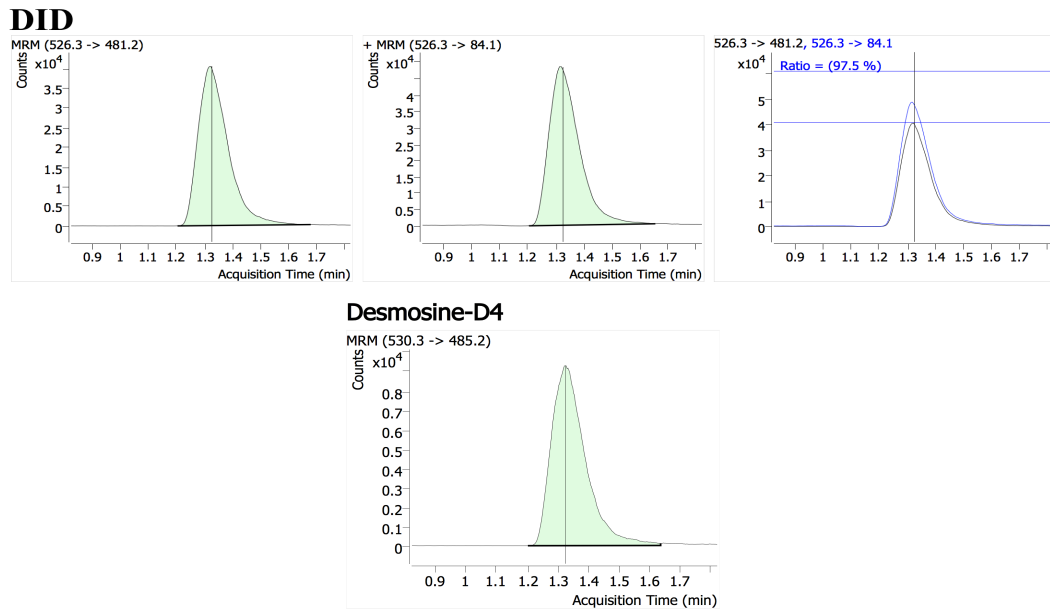


Figure 9. DID and desmosine-D₄ (40 ng/g, extracted)

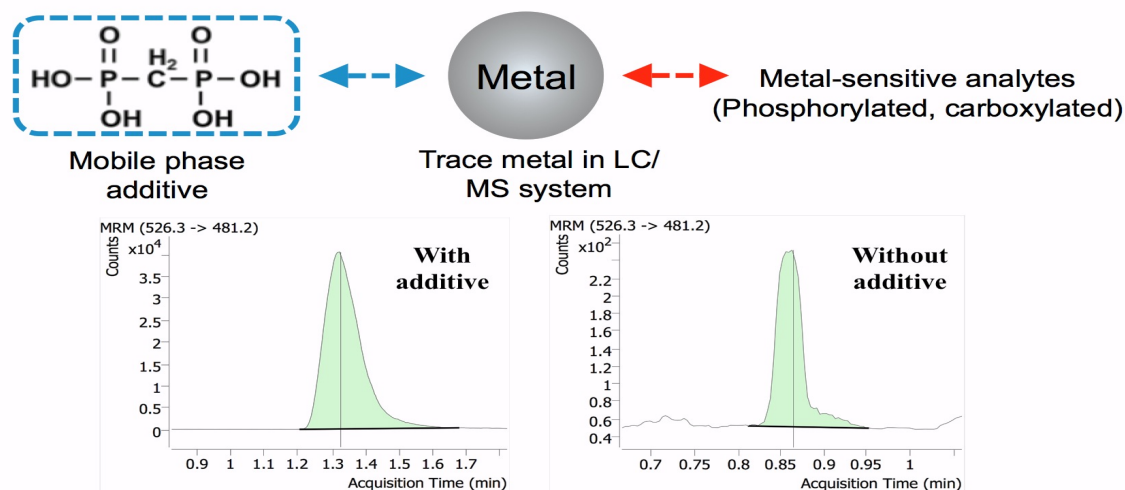


Figure 10. Chromatographs of DID with 5 μM medronic acid (left) and without 5 μM medronic acid (right) as a mobile phase additive [Top half of figure by J.J. Hsiao, O.G. Potter, T.W. Chu, Improved LC/MS Methods for the Analysis of Metal-Sensitive Analytes Using Medronic Acid as a Mobile Phase Additive, 2018, by permission of American Chemical Society]

In order to determine the specific MRM transitions for DID and desmosine- D_4 , Agilent Technologies MassHunter[®] Optimizer software was used. This program automates the selection of the most optimal precursor and transition ions and the optimal fragmentor and collision energy voltages for each precursor and transition ion. Automation of the optimization tasks occurred in the following order: a) the optimization of the fragmentor voltage to maximize precursor ion intensity, b) selection of the best product ions, and c) the optimization of the collision energies to maximize product ion intensity. Table 2 lists the optimized precursor and transition ions used for this study.

Following early unsuccessful attempts to optimize DID and desmosine- D_4 , it was decided that a non-ion-pair mobile phase additive was necessary. Medronic acid was chosen as a response to potential sensitivity issues when the structure of DID itself is considered, where the presence of multiple carboxylate moieties in the compound can lead to metal-analyte interactions (29-34). These carboxylate functional groups may potentially act as chelators, resulting in DID becoming “stuck” to transition metals or

other metallic impurities present within a sample, thereby limiting sensitivity and/or retention. Medronic acid is a phosphonation agent that only interacts with the metal in the LC and not the analytes of interest, precluding the need for traditional ion-pairing agents in this method. As mentioned above, medronic acid was added to the mobile phase at a concentration of 5 μM (1:1000 dilution) and, unlike traditional ion-pairing agents, does not persist in the LC–MS-MS system after use (29-34). Following the addition of medronic acid, there was a significant improvement in DID response, enough to allow the monitoring of two ion transitions for the native compound compared to just one MRM transition often cited in the literature (Figures 8, 9, and 10).

3.2 Neat and Extracted Calibration Curve of DID

Both un-extracted and extracted standard curve linearity was measured using the ratio of the analyte peak area to the internal standard peak area. The linear range was administratively set between 40 to 2000 ng/g in solid tissue for the purposes of this study. The limit of quantitation was set to the lowest calibrator concentration of 40 ng/g, while the upper limit of linearity was set to the high control concentration of 2500 ng/g. In order to verify proper calibration, three positive QC samples (with target concentrations interspersed among the linear range) along with a negative QC sample containing only the internal standard were subsequently analyzed. Correlation coefficients (r^2) for the calibration curve used to ascertain the linear range were > 0.995 when a weighting factor of $1/x$ was employed for un-extracted DID ($y = 0.002007x + 0.024771$, $n=8$) and for extracted DID ($y = 0.002037x + 0.004438$, $n=8$). Carryover was initially monitored by the use of blank injections of the mobile phase. The injection of a mobile phase blank following both un-extracted and extracted high control samples showed no carryover

contamination. Subsequently, a negative QC sample containing only the internal standard was injected after the un-extracted and extracted high control samples to monitor carryover every time the curve was run.

3.3 Chromatographic and Mass Spectral Separation of Desmosine and Isodesmosine

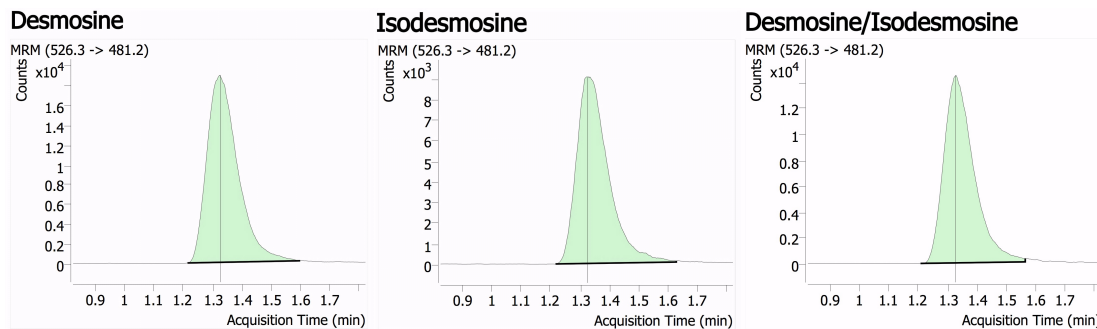


Figure 11. Chromatographs of extracted standards of desmosine (left), isodesmosine (middle), and combined desmosine/isodesmosine (right). Note the identical quantifier (major) transition ions as well as retention times.

Prior analytical methods have chromatographically separated desmosine from its structural isomer isodesmosine, however it was determined that such separation might not be justified with respect to its interpretative significance. Desmosine and isodesmosine concentrations are often reported as “desmosine/isodesmosine (DID)” as opposed to “desmosine” or “isodesmosine” individually, given that both are elevated in COPD to a very similar extent, and neither desmosine nor isodesmosine is associated with a particular disease apart from one another. Analytically, isodesmosine also shares the exact same MRM transitions as desmosine ($526.3 \rightarrow 481.2$ and 84.1 m/z) and is unable to be spectrally distinguished from desmosine. Baseline separation was not possible for desmosine and isodesmosine under the current method parameters, as their identical chromatographic and mass spectral characteristics cause both crosslinks to co-migrate (Figure 11).

3.4 Method Validation

3.4.1 General

The method was validated by evaluating linearity/calibration model, limits of detection, limits of quantitation, bias and precision, ionization suppression, enhancement, and extraction recovery, interferences (selectivity and specificity), dilution integrity, processed sample stability, and carryover. The general validation scheme was carried out based on ANSI/ASB Standard 036 (35) in plasma, urine, and solid tissue matrices. All instrumental and data analysis parameters were determined prior to the start of validation as part of method development and optimization.

3.4.2 Linearity/Calibration Model

Table 3. DID linearity evaluation

LEVEL	TARGET	SET 1	SET 2	SET 3	SET 4	SET 5	mean	Std Dev	CV	
1	40.0	44.36	44.07	42.62	42.98	42.30	42.72	0.90	2.12	
2	100.0	91.80	91.36	95.38	97.19	93.94	94.95	2.44	2.57	
3	500.0	481.84	489.41	479.33	478.94	500.65	488.36	9.19	1.88	
4	1000.0	996.58	996.39	1021.63	970.35	1000.40	997.56	18.23	1.83	
5	2000.0	2025.42	2018.77	2001.04	2050.54	2002.71	2016.41	20.13	1.00	
r^2		0.999	0.999	0.999	0.998	0.999	0.999	0.0004	0.045	
r^2 of mean values plotted:							0.9988			
Curve Applied:		<input checked="" type="checkbox"/> Linear	<input checked="" type="checkbox"/> 1/x	<input type="checkbox"/> Quadrat						

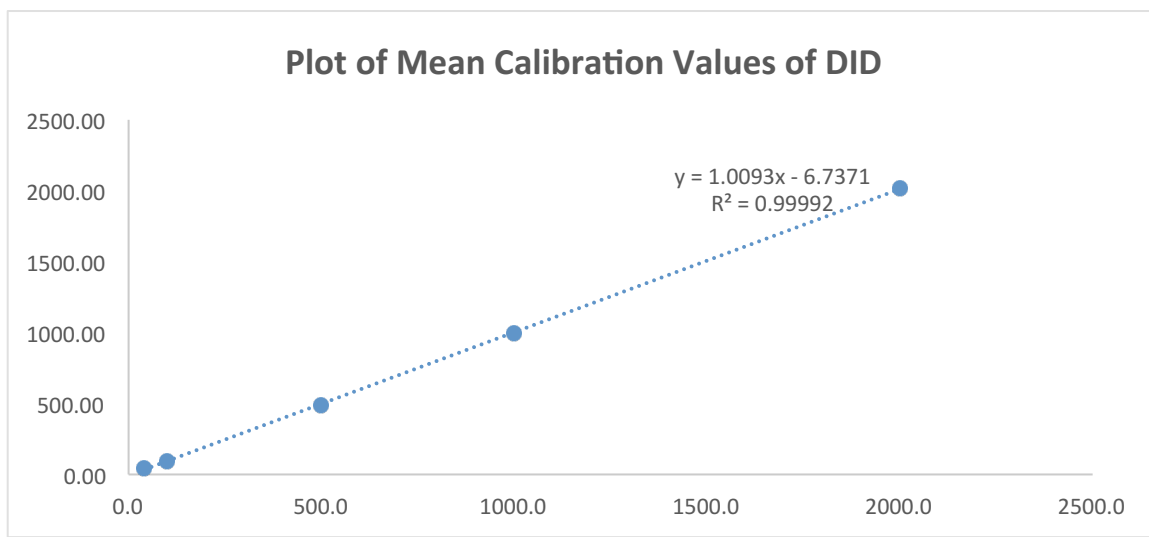


Figure 12. Plot of mean calibration values of DID (40 – 2000 ng/mL [ng/g])

Table 4. DID residual plot calibrator levels

Calib Residual Plot	<i>Calculate Residual Value From Target and Plot About Zero.</i>							
	LEVEL	TARGET	SET 1	SET 2	SET 3	SET 4	SET 5	
	1	40.0	4.36	4.07	2.62	2.98	2.30	
	2	100.0	-8.20	-8.64	-4.62	-2.81	-6.06	
	3	500.0	-18.16	-10.59	-20.67	-21.06	0.65	
	4	1000.0	-3.42	-3.61	21.63	-29.65	0.40	
	5	2000.0	25.42	18.77	1.04	50.54	2.71	

<i>Percentage From Target</i>							
LEVEL	TARGET	SET 1	SET 2	SET 3	SET 4	SET 5	
1	40	10.9	10.2	6.5	7.4	5.7	
2	100	-8.2	-8.6	-4.6	-2.8	-6.1	
3	500	-3.6	-2.1	-4.1	-4.2	0.1	
4	1000	-0.3	-0.4	2.2	-3.0	0.0	
5	2000	1.3	0.9	0.1	2.5	0.1	

(<20% for linear, 1/x) (<10% for quadratic)

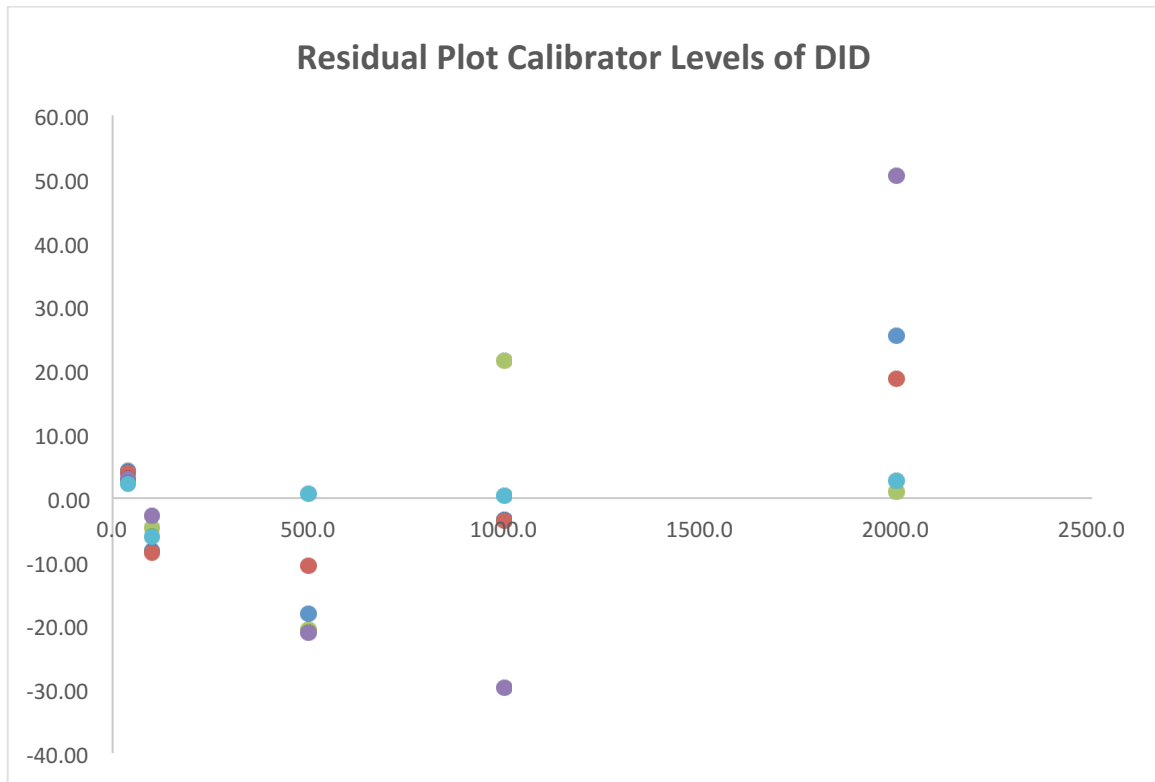


Figure 13. Residual Plot Calibrator Levels of DID

Linearity was evaluated through the analysis of five solid tissue calibration points over five analyses on separate days at the same time as accuracy and precision studies. The residual plots for linear and quadratic (with none, $1/x$ or $1/x^2$ weighting) regression models were assessed for quantitative suitability. The acceptability criteria for all calibration curves were set as a coefficient of determination (R^2) greater than 0.995 and $\pm 20\%$ accuracy on any individual calibration point, and with no more than one calibration point to be excluded.

Random distribution was best observed with a linear and weighted $1/x$ regression model for DID and was deemed appropriate for the quantification of DID across the chosen analytical range of 40 to 2000 ng/mL (ng/g). The combined data of the five non-zero concentrations evenly spaced across the calibration range with five replicates at each level analyzed in the same extraction (five replicates per level with five curves run sequentially) were used to establish the calibration model. The coefficient of determination (R^2) was >0.995 . All calibrators were within $\pm 20\%$ of their prepared concentration. The linearity and calibration model data are summarized in Figures 12 and 13 and Tables 3 and 4.

3.4.3 Limit of Detection (LOD) and Limit of Quantitation (LOQ)

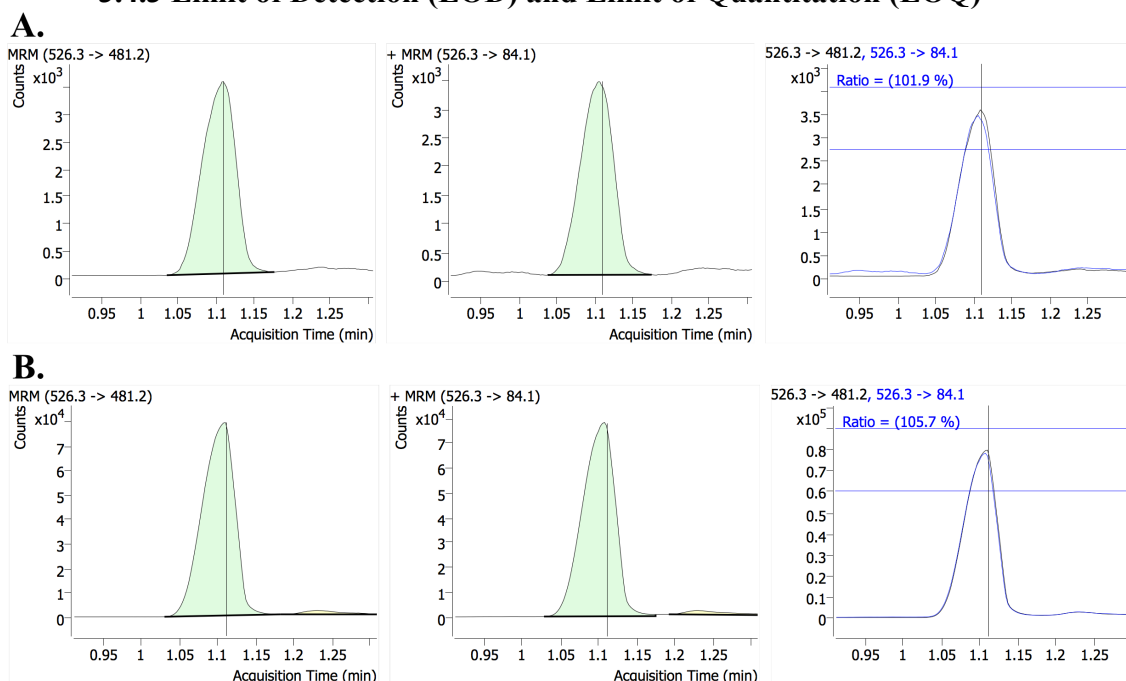


Figure 14. Extracted ion chromatogram for desmosine at a) its limit of detection and b) its limit of quantification

The LOD for desmosine was evaluated through the analysis of five replicates of a 20 ng/mL (ng/g) standard run in five separate extractions prepared in plasma, urine, and tissue matrices. All compounds had good chromatographic peak shape at the LODs. Signal-to-noise (S/N) for the LOD was calculated by the MassHunter[®] instrument software. All S/N ratios were greater than or equal to 4:1. MRM ion ratios were within \pm 20% and retention times were within 0.1 min compared to the average of all calibrators used (Figure 14). Consistent identification of DID was observed at the lowest concentration evaluated; DID may thus be identified in case samples below the validated LOD. No samples tested negative when fortified with a DID standard at the target concentration of the LOD and met all identification criteria. The method demonstrated suitable limits of detection for DID.

The LOQ of 40 ng/mL (ng/g) was verified by five replicates of a standard run in five separate extractions prepared in plasma, urine, and tissue matrices. All compounds had good chromatographic peak shape at the LOQ. S/N for the LOQ was also calculated by the MassHunter[®] instrument software. All S/N ratios were greater than or equal to 10:1. MRM ion ratios were within 20% and retention times were within 0.1 min compared to the average of all calibrators. The mean bias of quantitative results was within $\pm 20\%$ of their prepared concentration (Figure 14).

3.4.4 Bias and Precision

Table 5. Method performance

Analyte	Calibration range ng/mL ng/g*	LOD ng/mL ng/g	LOQ ng/mL ng/g	Control Levels ng/mL ng/g	Bias			Within-Run Precision (%CV)			Between-Run Precision (%CV)		
					150 ng/mL ng/g n=15	400 ng/mL ng/g n=15	800 ng/mL ng/g n=15	150 ng/mL ng/g n=6	400 ng/mL ng/g n=6	800 ng/mL ng/g n=6	150 ng/mL ng/g n=15	400 ng/mL ng/g n=15	800 ng/mL ng/g n=15
DID	40–2000	20	40	150, 400, 800	-4.24%	-1.63%	-1.95%	2.02%	1.51%	1.04%	4.47%	7.03%	3.94%

*If measured in solid tissue, units of ng/g are used

Bias and precision were evaluated in triplicate samples over different days in fortified plasma, urine, and solid tissue matrices at the low, medium, and high QC concentrations of 150, 400, and 800 ng/mL (or ng/g in solid tissue) respectively. Accuracy was calculated as the relative difference of the grand mean from the nominal value of DID. The acceptability criterion for accuracy was $\leq \pm 20\%$ for DID at each QC concentration. Precision was expressed as the CV. Two different types of precision studies were assessed during method validation: within-run precision (within-run CV) and between-run precision (between-run CV). The acceptability criterion for within-run and between-run CV precision studies was $\leq \pm 20\%$ for DID at each QC concentration.

The bias was between -4.24% and -1.63% of the prepared concentrations for DID across the low, medium, and high QC levels in fortified plasma, urine, and solid tissue

matrices. The within-run CV was between 1.04% and 2.02% for DID at all QC levels evaluated. Between-run CV was between 3.94% and 7.03% for DID at all QC levels evaluated. The CV for replicate injections of each QC level (at a minimum of six replicate injections) was between 1.04% and 2.02% for DID at all QC levels evaluated. Total CVs was $< \pm 20\%$. The bias and precision data are summarized in Table 5.

3.4.5 Ionization Suppression, Enhancement, and Extraction Recovery

Table 6. Summary of ionization suppression, enhancement, and extraction recovery studies

	DID			DESMOSINE-D ₄		
	A	B	C	A	B	C
	NEAT	POST ADD	EXTRACTED	NEAT	POST ADD	EXTRACTED
	80357	56422	51890	94054	73636	65947
	136112	57979	48430	161749	76354	67249
	159301	58507	44403	195824	81655	62071
MEAN	125257	57636	48241	150542	77215	65089
	Extraction Recovery (C/B*100)=		83.69942397			84.29579745
	Process Efficiency (C/A*100)=		38.5137185			43.23634327
	Ion Enhancement/Suppression (B/A*100)=		-53.98568273			-48.70877959

Ion suppression from potential matrix effects was assessed through a post-extraction addition method (35). Two different sets of samples were prepared, and DID and desmosine-D₄ peak areas of neat standards were compared to matrix samples fortified with neat standards after extraction. Set one consisted of neat DID prepared at the low and high QC concentrations (150 or 800 ng/mL [ng/g]) in plasma and solid tissue, each with desmosine-D₄. Neat DID was injected six times to establish a mean peak area for each concentration. Set two consisted of urine and solid tissue samples that were extracted in duplicate. After the extraction was complete, each matrix sample was fortified with the low or high QC concentrations of neat DID and desmosine-D₄. The average area of each set was used to estimate the suppression/enhancement effect at each concentration as follows for DID, desmosine-D₄, and the relative response for DID (quant ion/internal standard ion):

$$\text{Ionization suppression or enhancement (\%)} = \left(\frac{\bar{x}_{\text{Post Addition Sample Abundance}}}{\bar{x}_{\text{Neat Sample Abundance}}} \right) \times 100$$

DID and desmosine-D₄ demonstrated average suppression between -48% to -53%. Extraction recovery was between 83% to 84% for DID and desmosine-D₄. No impact was observed for the LOD, LOQ, or bias. This was verified by analyzing replicates in five separate extractions prepared in three different matrix sources (plasma, urine, and solid tissue). The use of an isotopically labeled internal standard compensated for any significant ion suppression or enhancement. Ionization suppression/enhancement/extraction recovery data are summarized in Table 6.

3.4.6 Selectivity, Specificity, Matrix Interferences, and Endogenous Interferences

Plasma, urine, and solid tissue samples were prepared and extracted to evaluate the selectivity of the method through interference studies. The specific samples are outlined below:

- 1) Matrix blanks fortified with DID at the same concentration as the carryover concentration (2500 ng/mL [ng/g]) without internal standard.
- 2) Matrix blanks fortified with internal standard only and no DID.
- 3) As patients with COPD may have extensive lung tissue breakdown, which may lead to the production of other elastin degradation products (36), the analytical method was evaluated for potential interferences using working solutions containing a total of 14 non-targeted analytes including amino acids, enzymes, and elastin constituents (Table 7).
- 4) 10 plasma, 10 urine, and 10 solid tissue samples from different sources that did not contain DID or internal standard.

There were no other significant matrix interferences from 10 different plasma, urine, or solid tissue sources that did not contain DID. There were no other interferences from the 14 analyzed analytes that may also be detected in those with COPD. There were no interferences from a high concentration of DID for the internal standards, and there were no interferences from the internal standard with DID. The method is specific for DID and desmosine-D₄.

Table 7. List of all exogenous compounds used for selectivity, specificity, matrix interferences, and endogenous compound interference studies (fortified at concentrations of 2500 ng/mL [ng/g])

Amino Acids, Enzymes, and Elastin Constituents:

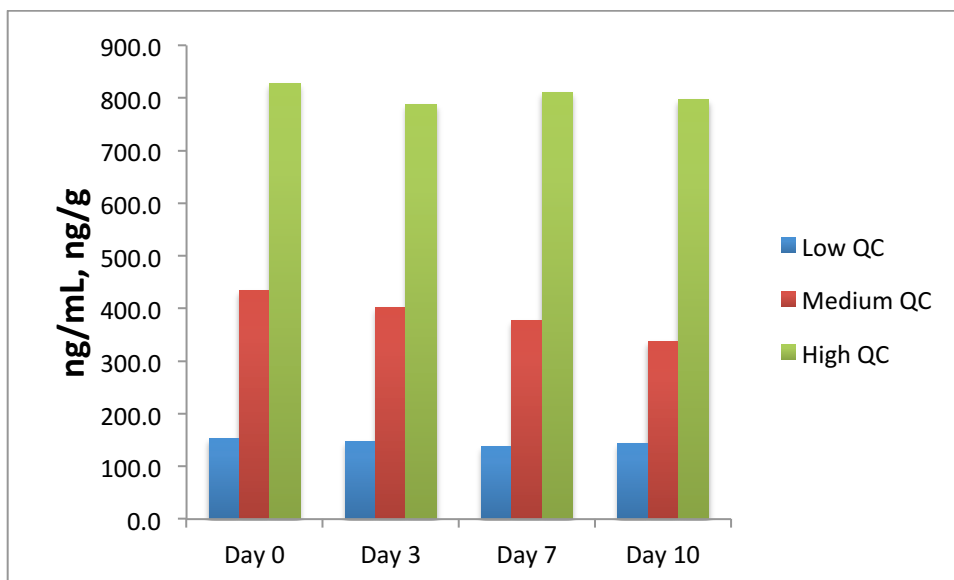
- L-Alanine
- L-Tyrosine
- L-Lysine
- L-Serine
- *trans*-4-hydroxy-L-Proline
- Chloramine-T (hydrate)
- 6-Oxo-DL-Norleucine
- Lysino Norleucine
- L-glutamine
- Hyaluronan
- Elastase
- Lipopolysaccharide
- Proteinase K
- Human lung elastin (unhydrolyzed and hydrolyzed)

3.4.7 Dilution Integrity

In cases of low specimen volume or potentially excessive DID concentrations that may be encountered, it was necessary to evaluate the effects of sample dilution using both ultrapure water and blank matrix (plasma, urine, and solid tissue). This was accomplished by establishing bias and within-run precision studies at dilution ratios of 1:2 (x2), 1:5 (x5), and 1:10 (x10) in plasma, urine, and solid tissue, respectively. All dilutions of fortified matrices met acceptance criteria as denoted in the bias and precision studies.

3.4.8 Processed Sample Stability

Table 8. Stability of DID over a period of 10 days



	Low QC (ng/mL, ng/g)	Medium QC (ng/mL, ng/g)	High QC (ng/mL, ng/g)
Day 0	153.8	435.3	828.1
Day 3	148.4	402.8	788.2
Day 7	137.3	377.0	810.3
Day 10	144.4	337.4	796.7

DID was evaluated for stability in fortified blank matrix (Table 8). Fortified samples were prepared at the low, medium, and high QC concentrations (150, 400, and 800 ng/mL [ng/g], respectively). With the goal of replicating an actual reinjection scenario, extracts were first injected on day 0 and, following batch completion, were allowed to sit in a temperature-controlled autosampler (5°C). Extracts were then re-injected on days 3, 7, and 10 post-extraction. The calculated concentrations in fortified QC samples containing DID remained within $\pm 20\%$ of their target concentrations from

day 0. It is important to note that authentic specimens may experience variable stability owing to sample conditions (fresh, fixed, decomposed, etc).

3.4.9 Carryover

Carryover was determined by the analysis of five extracted replicates. Extracted plasma, urine, and solid tissue samples were fortified and extracted at a concentration 2500 ng/mL (ng/g). Each mixture was bracketed by solvent vials containing a 95:5 mixture of ultrapure water and methanol. The solvents were evaluated for the presence of DID injected from the prior mixture; DID was not detected. Subsequently, a negative QC sample containing only the internal standard was injected after each extracted carryover sample to monitor carryover every time a calibration curve was run during the bias and precision studies. No DID carryover response greater than the LOD area ratio was observed following the injection of extracted plasma, urine, and solid tissue at concentrations of 2500 ng/mL (ng/g).

3.5 Re-Analysis of Human Plasma, Urine, and Sputum Samples

Table 9. DID Measurements in human plasma, urine, and sputum – Current method

Compartment	Group	Day 1 (Initial)	Day 14	Day 28	Day 35
Sputum (Total desmosine – ng/mg protein; % change)	HA	15.8 ± 2.40 (0%) [7]	14.4 ± 2.24 (-9.27%) [7]	11.7 ± 1.24 (-29.8%) [7]	N/A
	P	19.0 ± 3.03 (0%) [8]	12.9 ± 2.00 (-38.2%) [8]	15.9 ± 1.61 (-17.8%) [10]	N/A
Urine (Free desmosine – ng/mg creatinine; % change)	HA	16.8 ± 4.56 (0%) [12]	16.2 ± 2.33 (-3.63%) [10]	15.4 ± 1.90 (-8.69%) [11]	11.9 ± 1.64 (-34.1%) [11]
	P	13.9 ± 3.66 (0%) [11]	10.3 ± 2.17 (-29.7%) [10]	13.5 ± 2.45 (-2.92%) [12]	15.2 ± 2.55 (+8.93%) [13]
Urine (Total desmosine – ng/mg creatinine; % change)	HA	27.7 ± 4.52 (0%) [12]	31.7 ± 4.12 (+13.4%) [10]	30.7 ± 2.32 (+10.2%) [10]	24.9 ± 3.19 (-10.6%) [11]
	P	26.6 ± 4.56 (0%) [12]	23.5 ± 6.20 (-12.4%) [11]	28.8 ± 5.92 (+7.94%) [12]	29.1 ± 5.14 (+8.98%) [13]
Plasma (Total desmosine – ng/mL; % change)	HA	6.30 ± 1.80 (0%) [5]	4.17 ± 0.74 (-40.7%) [7]	2.52 ± 0.43 (-85.7%) [7]	3.70 ± 0.22 (-52.0%) [4]
	P	4.76 ± 1.77 (0%) [5]	5.98 ± 1.83 (+22.7%) [5]	7.52 ± 1.44 (+44.9%) [5]	6.55 ± 1.49 (+31.7%) [7]

Values are mean ± standard error of the mean.

Numbers in parenthesis indicate percent change in desmosine concentration from day 1.

Numbers in brackets indicate N.

Abbreviations: HA, hyaluronan; P, placebo; N/A, not applicable.

Table 10. DID Measurements in human plasma, urine, and sputum – Previous method

Compartment	Group	Day 1	Day 14	Day 28	Day 35
Sputum (ng/mg protein)	H	0.96 ± 0.67 (6)	0.49 ± 0.40 (6)	0.18 ± 0.12 (7)	N/A
	P	0.31 ± 0.22 (5)	1.4 ± 0.85 (6)	0.24 ± 0.093 (7)	N/A
Urine (Free DID) (ng/mg creatinine)	H	16 ± 1.3 (13)	16 ± 1.9 (12)	15 ± 1.2 (12)	14 ± 1.1 (12)*
	P	13 ± 1.2 (13)	13 ± 1.4 (13)	13 ± 1.3 (12)	13 ± 1.3 (13)
Urine (Total DID) (ng/mg creatinine)	H	31 ± 2.6 (13)	31 ± 3.9 (12)	30 ± 2.4 (12)	29 ± 2.4 (12)
	P	27 ± 2.7 (13)	26 ± 2.9 (13)	27 ± 2.7 (12)	28 ± 2.7 (13)
Plasma (ng/ml)	H	0.61 ± 0.038 (13)	0.62 ± 0.043 (13)	0.64 ± 0.043 (13)	0.62 ± 0.047 (13)
		0.61 ± 0.040 (13)	0.61 ± 0.048 (13)	0.59 ± 0.051 (13)	0.58 ± 0.046 (13)
	P	0.61 ± 0.040 (13)	0.61 ± 0.048 (13)	0.59 ± 0.051 (13)	0.58 ± 0.046 (13)
		0.61 ± 0.040 (13)	0.61 ± 0.048 (13)	0.59 ± 0.051 (13)	0.58 ± 0.046 (13)

Values are mean ± standard error of the mean.

Numbers in parentheses indicate n.

*p = 0.035 vs day 1.

Abbreviations: DID, desmosine and isodesmosine; H, hyaluronan; P, placebo.

A 2-week clinical trial of aerosolized hyaluronan (HA) in COPD by Cantor et al. showed a rapid reduction in lung elastic fiber breakdown as measured by sputum levels of desmosine (37). The same investigators conducted an additional 28-day randomized, double-blind, placebo-controlled, phase 2 trial of HA involving 27 subjects with a homozygous genotype for alpha-1-antiprotease deficiency-mediated COPD, with desmosine quantified in plasma, urine, and sputum by a previously described LC–MS–MS method for desmosine quantification (17, 31). As further validation of the method, these samples were reanalyzed under the currently described parameters and the results were compared. The results from this trial – along with our reanalysis of these samples

(Tables 9 and 10) – indicate a negative correlation of free urine desmosine and a marked decrease in total sputum desmosine following HA administration. However, while the authors of the previous study found no significant decreases in plasma desmosine in the HA group, there was a decrease of plasma desmosine in this group following reanalysis in our method. Several factors including a larger sample volume, a significant time delay between analyses, matrix-dependent stability of desmosine, changes in creatinine or protein content, or differences in analytical sensitivity (including LOD and LOQ) between methods may have contributed to the discrepant plasma results, which have been shown in the past to be higher in those with COPD compared to healthy controls (31). Additionally, no significant reductions in urine, sputum, or plasma desmosine were seen in the placebo groups (17, 37).

3.6 Hamster Lung Morphology

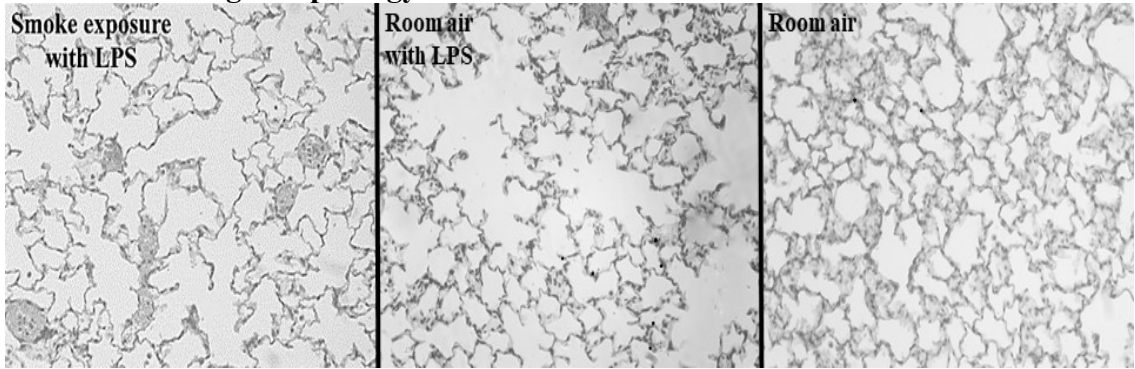


Figure 15. The lung from an animal treated with cigarette smoke and LPS (left) has greater airspace enlargement than one from the group given LPS alone (center). A room air control lung (right) is shown for comparison. Original magnification for all 3 photomicrographs: 100x.

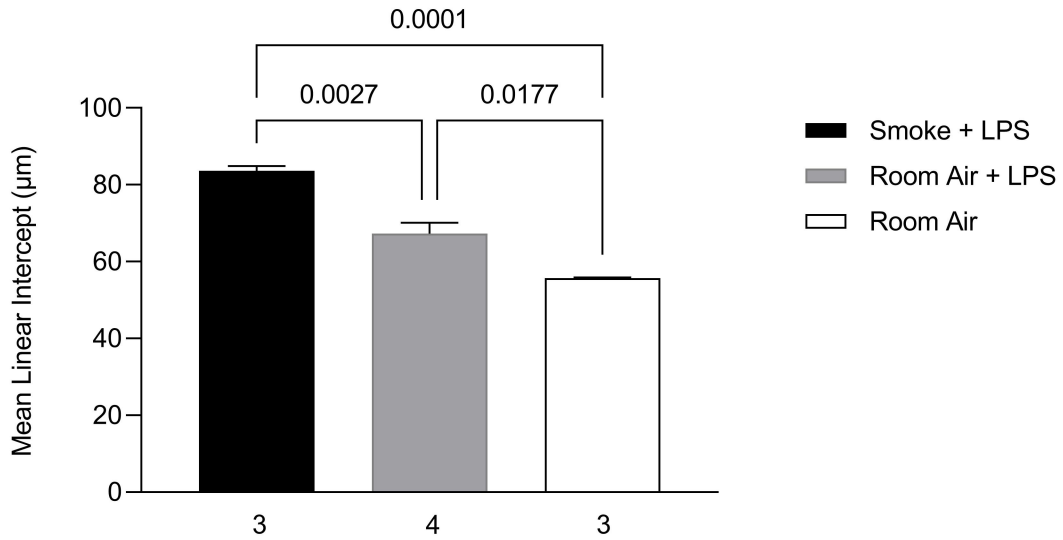


Figure 16. Animals treated with smoke and LPS had a significantly increased MLI compared to those given LPS alone and room air controls. Numbers below bars indicate N. T-bars denote SEM.

Microscopic examination of the lungs and measurement of MLI were performed 24 hrs following LPS administration. Hamsters treated with smoke and LPS had a mild to moderate degree of pulmonary emphysema (Figure 15) and a significantly greater MLI than that of both the LPS only group (83.6 vs. 67.3 µm; $p=0.0027$; Figure 16) and room air controls (55.7 µm; $p=0.0001$). Animals given LPS alone showed less airspace enlargement than those receiving smoke and LPS, but also had a significantly increased MLI compared to controls ($p=0.0177$).

3.7 Hamster BALF Cell Content

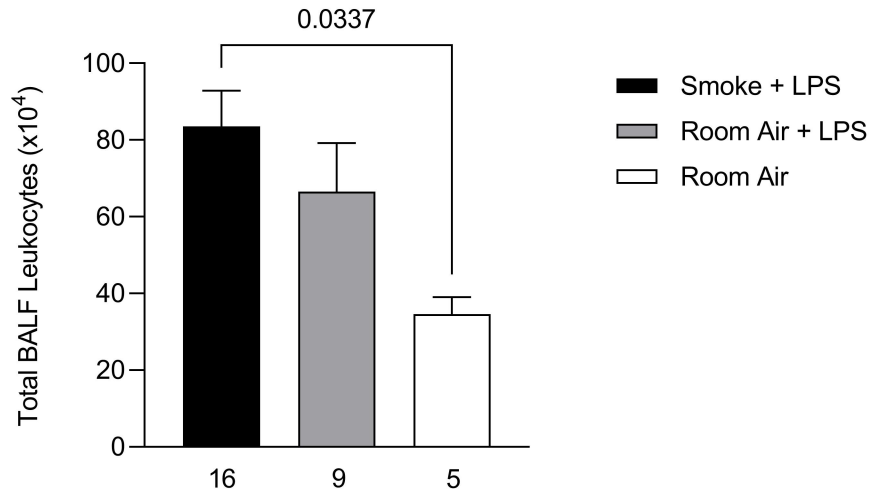


Figure 17. Animals treated with cigarette smoke and LPS showed a significant increase in total BALF leukocytes compared to room air controls. Numbers below bars indicate N. T-bars denote SEM.

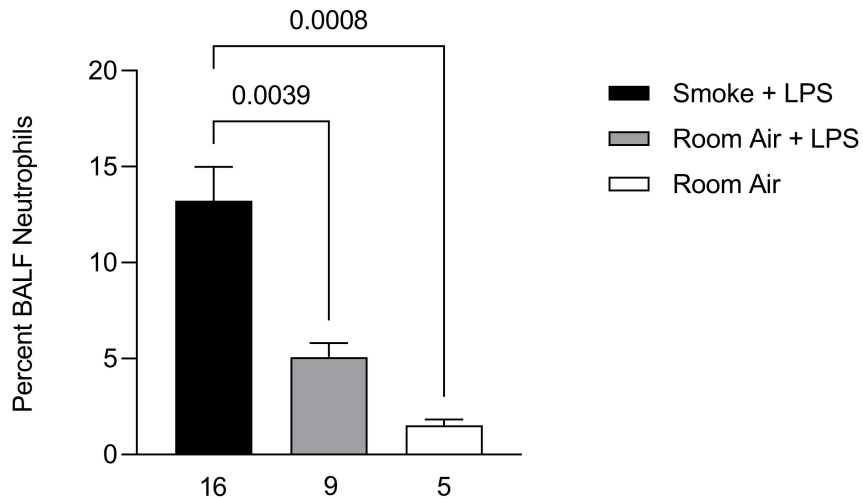


Figure 18. Animals treated with cigarette smoke and LPS showed a significant increase in percent BALF neutrophils compared to those given LPS alone and room air controls. Numbers below bars indicate N. T-bars denote SEM.

Measurement of total BALF leukocytes and percent BALF neutrophils were performed 24 hrs after LPS treatment. Animals receiving smoke and LPS showed a significant increase in total BALF leukocytes compared to room air controls (83.5 vs.

34.6 x 10⁴ cells; p=0.0337; Figure 17), whereas the difference between the LPS only group and controls was not significant. BALF neutrophils were also significantly increased in animals given smoke and LPS compared to the LPS only group and controls (13.2 vs. 5.1 vs. 1.5 percent; p=0.0039 and p=0.0008, respectively; Figure 18). In contrast, the LPS only group did not show a significant increase from controls.

3.8 Free Hamster Lung DID

Table 11. Comparison of free DID levels in fresh and fixed hamster lung tissue

Group	Fresh	Fixed	P-value
Smoke + LPS	391 ± 121 (3)*	327 ± 60.5 (3)	>0.99
Room Air + LPS	76.1 ± 27.6 (3)	110 ± 13.3 (3)	>0.99
Room Air	ND (2)	ND (2)	-

*Results are expressed as ng/g wet lung (mean ± SEM). Numbers in parenthesis indicate N. ND: not detected.

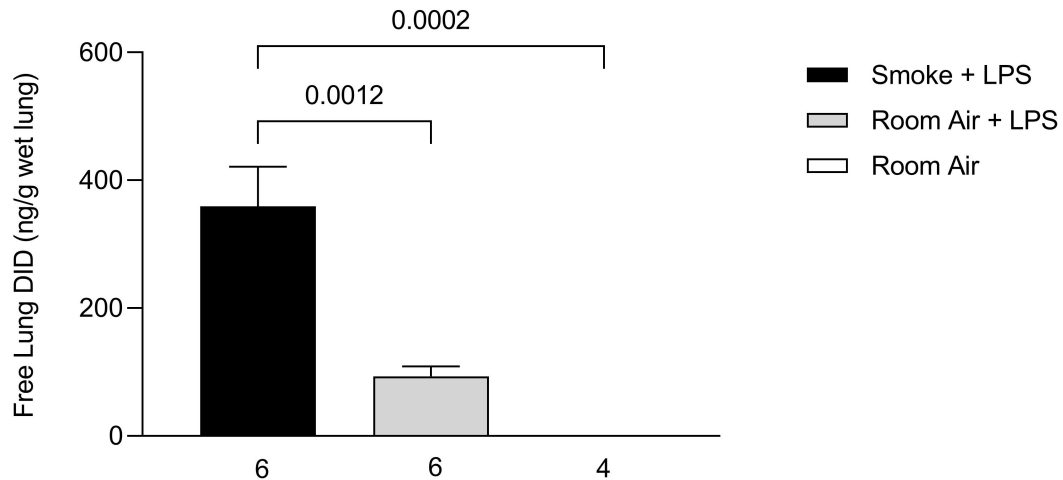


Figure 19. Animals treated with cigarette smoke and LPS showed a significant increase in free lung DID compared to both the LPS only and room air control groups. Results include both formalin-fixed and fresh lung tissues. Numbers below bars indicate N. T-bars denote SEM.

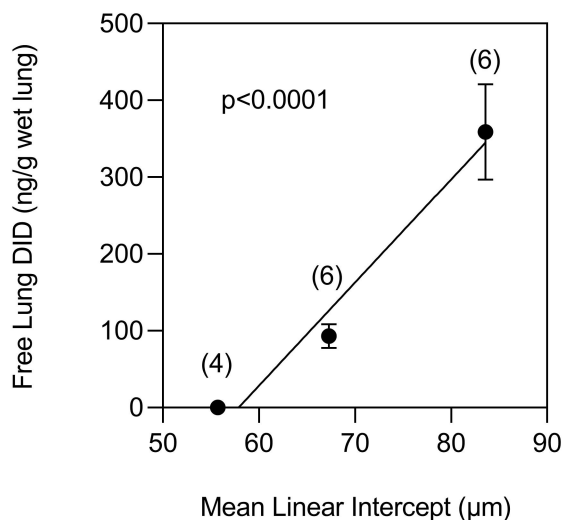


Figure 20. There was a significant positive correlation between MLI and free lung DID in both formalin-fixed and fresh lungs ($p<0.0001$). MLI values are the means from Figure 16. Numbers in parentheses indicate N. T-bars denote SEM.

To determine the amount of elastic fiber injury, lungs were measured for free DID 24 hrs after LPS administration. As shown in Table 11, there was no significant difference in free DID between fresh and formalin-fixed lungs. Animals treated with smoke and LPS had significantly higher levels of free DID compared to those given LPS alone (359 vs. 93.1 ng/g wet lung $p<0.0012$; Figure 19). The room air control group did not have detectable levels of free DID. As shown in Figure 20, there was a significant positive correlation between free DID and MLI ($p<0.0001$).

3.9 Human Lung Morphology

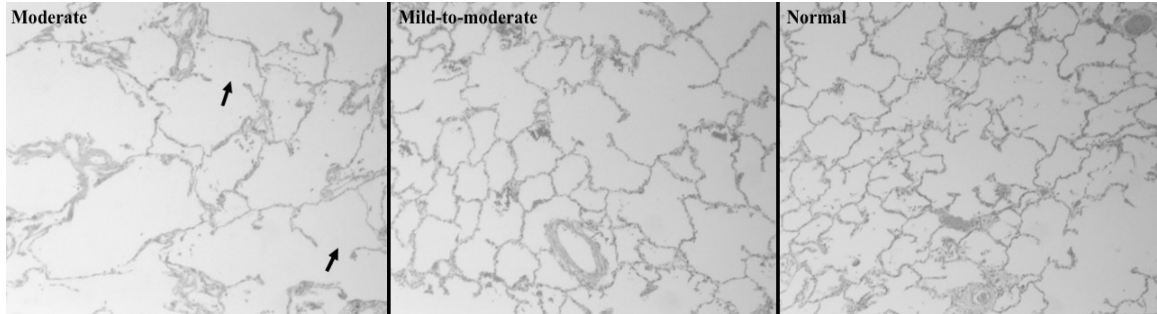


Figure 21. (Left to Right) Photomicrographs of specimens showing moderate, mild to moderate, and no pulmonary emphysema. The one with moderate airspace enlargement had dilated alveolar walls with focal areas of rupture (arrows). Original magnification for all 3 photomicrographs: 40x.

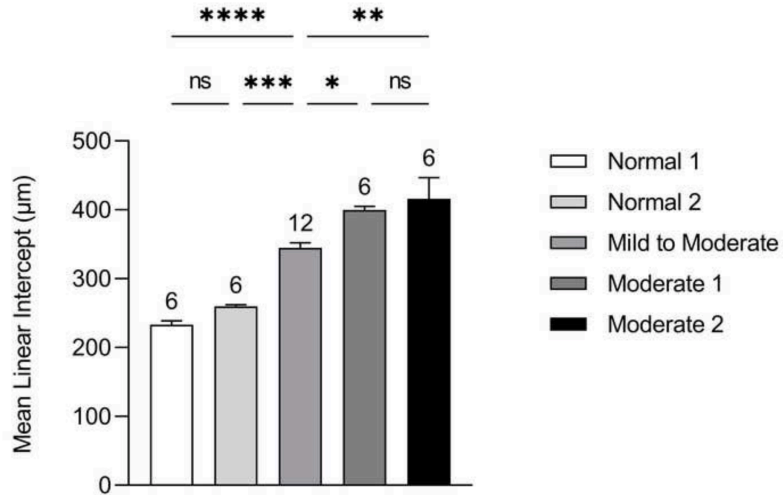


Figure 22. The lung tissues with moderate emphysema had a significantly greater MLI than the one with mild to moderate disease, but there was no significant difference between the two with moderate airspace enlargement. Numbers above bars indicate N. T-bars denote SEM.

The three samples procured from individuals with COPD showed varying degrees of emphysema (Figure 21). Airspace enlargement in those with moderate disease was accompanied by thinning of and rupture of alveolar walls. As shown in Figure 22, the MLI of the COPD specimens was significantly greater than that of the normal group. The lung tissues with moderate emphysema also had a significantly higher MLI than the one

with mild to moderate disease. However, the difference between the two with moderate airspace enlargement was not significant.

3.10 Human Lung DID

Table 12. Clinical histories associated with the human lung tissue specimens

Lung Specimen	Age	Gender	Smoking History	Cause of Death	Primary Disease	Other Diseases	Tissue Recovery Interval (hrs)
Normal 1	74	M	Unknown	Cardiogenic Shock	Cardiomyopathy	Diabetes/Renal Failure	24
Normal 2	89	M	Unknown	Septic Shock/GI Bleed	Congestive Heart Failure	Dementia/Severe Atherosclerosis	96
Mild to Moderate	79	M	Unknown	Cardiogenic Shock	Congestive Heart Failure	COPD/Prostate CA	208
Moderate 1	68	M	Current/2 packs x 50 years	Cardiogenic Shock	Congestive Heart Failure	COPD with Dyspnea/Diabetes	24
Moderate 2	79	F	Current/pack years unknown	Ruptured Aortic Aneurysm	Aortic Aneurysm	COPD/Severe Atherosclerosis	46

Table 13. Comparison of free DID levels in fresh and fixed human lung tissue

Group	Fresh	Fixed
Normal 1	N/A	11.2 ± 1.9 (10)*
Normal 2	N/A	11.3 ± 1.8 (10)
Mild-to-moderate	83.3 ± 7.6 (10)	70.7 ± 7.8 (10)
Moderate 1	484.9 ± 18.5 (10)	460.5 ± 23.8 (10)
Moderate 2	N/A	1449.3 ± 163.0 (10)

*Results are expressed as ng/g wet lung (mean ± SEM). Numbers in parenthesis indicate *N*. N/A: not applicable.

Table 14. Comparison of total DID levels in fresh and fixed human lung tissue

Group	Fresh	Fixed
Normal 1	N/A	30.5 ± 2.5 (10)*
Normal 2	N/A	27.7 ± 2.8 (9)
Mild-to-moderate	252.7 ± 12.3 (10)	295.1 ± 11.9 (10)
Moderate 1	854.3 ± 25.8 (10)	818.7 ± 22.5 (10)
Moderate 2	N/A	2812.5 ± 209.8 (10)

*Results are expressed as ng/g wet lung (mean ± SEM). Numbers in parenthesis indicate *N*. N/A: not applicable.

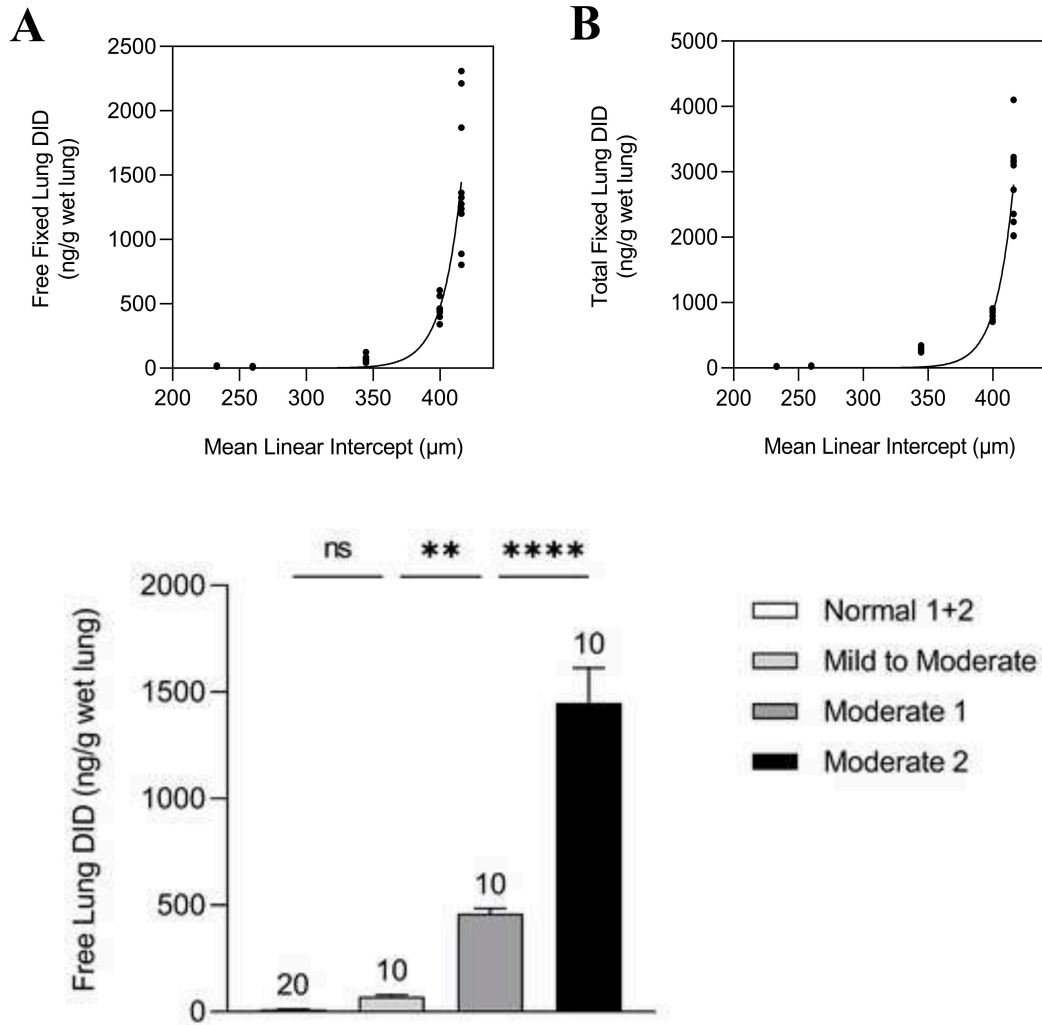


Figure 23. (Upper) The nonlinear regression curves indicate that accelerated elastin breakdown is associated with an MLI above 400 μm . (Lower) The level of free DID was significantly increased in tissues with moderate emphysema compared to all other groups. Numbers above bars indicate N. T-bars denote SEM

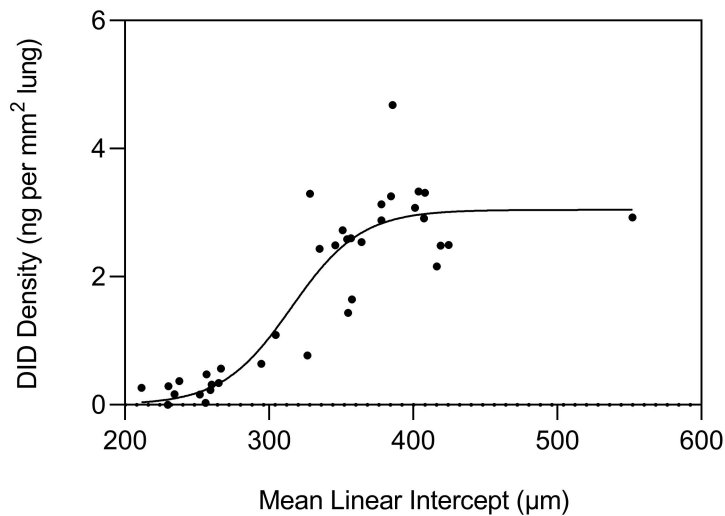
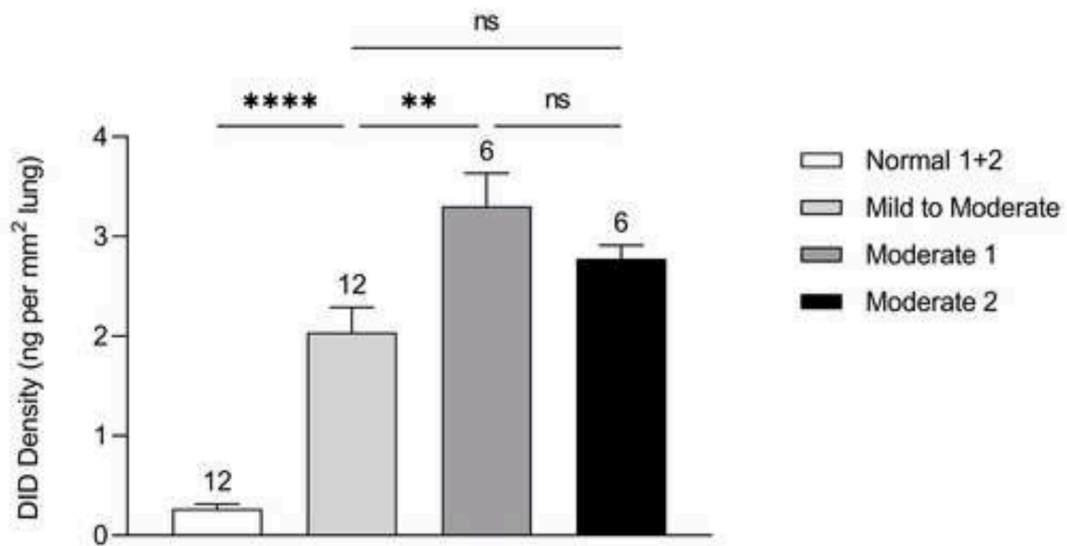


Figure 24. (Upper) A progressive increase in DID density was associated with the continued development of pulmonary emphysema. Numbers above bars indicate N. T-bars denote SEM. (Lower) A nonlinear curve (plateau followed by one phase association) more closely fit the data and was used to model the proposed relationship between DID density and MLI.

The use of fixed tissue was justified by a previous study from this laboratory showing no significant difference in free and total DID levels between formalin-treated and fresh material. Measurements performed on multiple fixed samples from each specimen indicated a positive correlation between free and total DID and the extent of airspace enlargement ($p < 0.0001$). The amount of free DID was markedly increased in

tissues with moderate emphysema compared to all other groups (Figure 23, Tables 12, 13 and 14). These results are consistent with accelerated elastin breakdown in lungs with an MLI greater than 400 μm .

There was a progressive increase in DID density associated with the continued development of pulmonary emphysema (Figure 24). Although linear regression showed a significant positive correlation between crosslink density and MLI ($p < 0.0001$), a nonlinear curve (plateau followed by one phase association) more closely fit the data ($r^2 = 0.82$ vs. 0.68) and was used to model this relationship. The curve indicated that DID density markedly increased beyond 300 μm and leveled off around 400 μm (Figure 24). This pattern is consistent with a robust remodeling of elastic fibers due to the mechanical strain of airspace enlargement, followed by a postulated “decompensation” phase in which elastin degradation overwhelms the repair process, thus compromising the structural integrity of alveolar walls.

CHAPTER 4:

DISCUSSION

4.1 Preface

We hypothesized that DID is a potential biomarker for emphysematous changes in COPD. We additionally hypothesized that increases in DID in biological fluids correlate with the degree of pulmonary airspace enlargement, that the level of peptide-free DID in lung tissue is a sensitive and specific marker for pulmonary emphysema, and that the density of DID in lung tissue may vary with mechanical strain imposed by airspace enlargement.

4.2 Evaluation of Current LC–MS Based Assays for Desmosine Analysis and Adoption of Non Ion–Paired Reverse–Phase High–Performance Liquid Chromatography

In part, concerns for the acceptance of DID as a valid biomarker have often been related to current limitations of analytical methodology. However, the results of several clinical trial studies have yielded promising results and have augmented the arguments for inclusion of DID as a valid biomarker of COPD (30, 38–39). Despite this, there is still much to be desired with some of the current published analytical methods, as they typically only measure DID in fluids, predominantly urine, which are often interpreted as ‘per se’ indicators of elastin degradation. Thus, it was of interest to the authors to develop an optimized LC–MS-MS method in lung tissue, as this matrix could potentially provide insight into COPD disease progression as well as the extent tissue degeneration and airspace enlargement that is characteristic of COPD, potentially fulfilling the remaining

criteria for DID's acceptance as a valid biomarker. It was further hypothesized that such measurements may also be useful in the arena of medicolegal death investigation, where DID may serve as a tool in the postmortem assessment of airway injury during autopsy that is otherwise not anatomically or histologically observable. Such measurements could potentially aid a pathologist in attributing acute or chronic lung disease toward the cause and manner of death. However, more studies are needed to fully characterize the role of DID in medicolegal death investigation.

Our results utilizing non ion-paired reverse-phase high-performance liquid chromatography (NIP-RPC) in the analysis of DID have the potential to expand the current methodology in the literature where ion-pairing agents are often employed. Various bioanalytical techniques have been previously reported for the measurement of DID, including radioimmunoassay (RIA), high-performance liquid chromatography (HPLC), and capillary zone electrophoresis (40). However, techniques utilizing LC-MS-MS have been reported as a more sensitive and specific means of quantification, and have gained wider favor for DID analysis in the clinical setting (31-34, 41-44).

In LC-MS-MS, the advantage of this technique lies with using two quadrupole analyzers with a collision cell. The production of unique transition ions in the collision cell reduces the possibility of interferences and misidentification of the analyte in question, owing to the isolation of the precursor ion in the first quadrupole and determination of the presence of the unique transition ions related only to that single precursor (27). This technique by which specific ions are produced greatly improves sensitivity, specificity, and reduces potential ion suppression due to interfering compounds that may have the similar masses, but not the same mass-to-charge ratios.

Furthermore, confidence in identification is improved as the mass spectral characterization is also dependent on instrumental parameters unique to isolating and fragmenting specific ions at specific fragmentor voltages that yields the highest signal abundance of those specific ions, as is often utilized for quantitative analysis. This is amply demonstrated by the lack of any visual interferences in our results of un-extracted standards and from extracted tissue, where matrix effects may be more prominently displayed in single quadrupole systems or other types of analytical techniques where the same degree of separation and identification cannot be achieved. In addition, the polar/hydrophilic nature of DID lends itself favorably to LC–MS and LC–MS-MS based assays where a range of compounds of varying polarities can be analyzed and quantified with relative ease by ESI.

However, even with tandem mass spectrometry, much of the published methodology for DID analysis utilizes ion-pairing agents extensively. Ion-pair chromatography has been used for the separation of ionized compounds that are not well-retained using conventional reverse-phase chromatography. The retention mechanism of ion-pairing is based on the interactions formed between ionic solutes and ion-pairing reagent adsorbed on stationary phase (45–50). Without the addition of ion-pairing agents to mobile phases, quantitative analysis of ionized analytes becomes nearly impossible due to poor retention and sensitivity of the target analytes (29-34). More recently, the high purity and robustness of many reverse-phase columns on the market often preclude the need for ion-pairing agents, but the pyridinium ring, trivalent crosslinks, and multiple carboxylate moieties in the structure of DID present analytical challenges and difficulties in chromatographic separation, and have led investigators to use ion-pairing agents in an

attempt to produce better retention of the compound on reverse-phase columns with varying results (31–32, 34, 42–44).

Ion-pairing has also been heavily utilized for the separation of desmosine and isodesmosine. Chromatographic separation of structural isomers is often fraught with difficulties even with tandem mass spectrometry (27) and requires extensive analytical development in order to achieve baseline separation. Prior methods do not separate these crosslinks without sacrificing chromatographic run time, and current technology does not allow for mass spectral separation owing to identical precursor and transition ions for both crosslinks (Figure 11). In all cases, chromatographic separation of desmosine and isodesmosine in the previously described methods was achieved with extensive gradient elution; run times averaged between 10 to 30 min per injection. One novelty of this method is its short chromatographic run time, which is significantly shorter than previously published methods. Longer run times for the purposes of separating isodesmosine from desmosine, which may not provide additional diagnostic or interpretive value, are not suitable for the higher throughput analyses needed in clinical trials involving large numbers of samples. Additionally, desmosine and isodesmosine concentrations are often reported as “desmosine/isodesmosine” (DID) as opposed to “desmosine” or “isodesmosine” individually, given that both are elevated in COPD to a very similar extent, and neither desmosine nor isodesmosine is associated with a particular disease apart from one another.

There are additional disadvantages to ion-pairing agents, which stem predominantly from contamination of the column and the mass spectrometer, which serves in preventing the utilization of other applications due to ion suppression effects

and other analytical interferences. Furthermore, the regeneration of the starting ion-pair distribution across a column following gradient elution has been long recognized as a major disadvantage to ion-pair chromatography owing to long column equilibration times required to be effective. Often, post-run equilibration times are longer than the chromatographic separation, and insufficient post-injection times may lead to variable quantitative results from method-to-method or laboratory-to-laboratory (50). Long run times also prevent the possibility of high throughput analysis, which may become necessary as more clinical trials are conducted on COPD patients. Finally, laboratories operating under strict budgets may not have the ability to dedicate instrumentation only to applications that use ion-pairing agents; this may be a problem when other applications and methods are desired where ion-pairing isn't needed, or whose method development and validation would be poorly executed due to residual ion-pairing interferences.

One potential LC alternative in the analysis of DID includes hydrophilic interaction liquid chromatography (HILIC), but no such methods specific to DID utilizing HILIC columns have been published to date. The relative expense and technical expertise needed to properly implement HILIC columns may be factors that have prevented such methods from being published. For example, HILIC LC-MS and LC-MS-MS experiments are often fraught with challenges related to the chromatography of charged analytes. Often, these analytes suffer from poor peak shape that can only be resolved with either a flush of the LC system with a strong metal chelator such as ethylenediaminetetraacetic acid (EDTA), or through the addition of EDTA to the mobile phase. Unfortunately, this suffers the same consequences as other traditional ion-pairing agents (29-34).

Another potential instrumental alternative is gas chromatography-mass spectrometry (GC–MS) following bistrifluoroacetamide-trimethylsilyl (BSTFA–TMS) derivatization, a technique that has been long considered the “gold standard” for the quantitative analysis of amino acids (51), though no attempts have been made to analyze DID in this manner (52–54). Such pre-column GC–MS derivatization techniques bring disadvantages in terms of lengthy method development, analytical sensitivity issues, interferences with other non-derivatized applications, and instrument maintenance.

4.3 Free Lung Desmosine: A Potential Biomarker for Elastic Fiber Injury in Pulmonary Emphysema

To further establish the usefulness of DID as a biomarker of elastic fiber breakdown, we demonstrated a possible correlation between its concentration in the lungs of hamsters treated with cigarette smoke and LPS and the degree of pulmonary airspace enlargement as visualized through histological analysis and as measured by the MLI method. Furthermore, we also analyzed plasma, urine, and sputum samples from a recently completed clinical trial of a novel treatment for COPD (17, 37). The results are consistent with a previously described method for DID quantification, and it also demonstrates that DID may serve as an effective real-time measure of COPD drug efficacy. Through providing faster results on the efficacy of potential COPD drug candidates, DID can also be used as a “decision-point” for further clinical trial development.

The model of pulmonary emphysema used in the animal study depends on the interaction of short-term cigarette smoke exposure with the proinflammatory effects of LPS. A number of studies indicate that brief treatment with smoke alone is not associated

with significant pulmonary injury and may only result in airspace enlargement if there is secondary lung inflammation (55–58). One of the reasons why actual lung damage from short-term secondhand smoke exposure alone is difficult to ascertain may relate to the lack of sensitive measures of alveolar wall injury. From a public health perspective, the measurement of free lung DID may permit earlier detection of disease, thereby increasing our understanding of the harmful effects of even limited contact with secondhand smoke and other types of environmental pollutants such as ozone and nitrogen dioxide. The morphological changes produced by the combination of cigarette smoke and LPS may involve activation of shared proinflammatory pathways. Smoke-induced release of various inflammatory mediators could intensify the influx of leukocytes associated with LPS administration.

The increase in BALF neutrophils seen in lungs treated with both smoke and LPS reflects enhanced migration of these cells from the pulmonary capillary bed to the alveolar space. It was previously shown that cigarette smoke-induced secretion of elastase by neutrophils facilitates their dissociation from adhesion molecules that tether them to capillary endothelium (59). Pre-exposure to cigarette smoke may therefore enhance the ability of neutrophils to respond to chemotactic stimuli generated by LPS administration.

The continued secretion of elastase by neutrophils migrating into the extravascular compartment would degrade elastic fibers, causing alveolar wall distention and rupture. The resulting changes in the distribution of mechanical forces could cause the fibers to undergo further fragmentation, enhancing the release of elastin crosslinks. Consequently, the level of free lung DID may be a sensitive indicator of

microarchitectural changes in alveolar walls prior to the development of visually apparent airspace enlargement. In particular, this biomarker may have diagnostic potential in autopsy cases where gross and microscopic findings are not definitive for pulmonary emphysema, or the necessary apparatus to properly inflate the lungs for MLI measurements are unavailable. The availability of LC–MS-MS equipment in forensic pathology laboratories suggests the possible early adoption of the biomarker to rule out early lung changes associated with undiagnosed COPD as a contributing factor in mortality. Determining the presence of occult lung disease would be especially useful in cases where extensive cardiovascular disease may be fatally exacerbated by even modest reductions in pulmonary gas exchange.

In comparison to other proposed biomarkers, structural components such as DID may be better indicators of pulmonary emphysema than inflammatory mediator pulmonary emphysemas because they reflect emerging abnormalities in mechanical forces within the lung (60–61). As shown by computer models simulating airspace enlargement in the lung, the interaction of various submicroscopic processes can lead to repeating patterns of stress-induced injury at different levels of scale (62–63). Loss of elastin crosslinks and separation of peptide chains at the molecular level may be reflected by microscopic fragmentation of elastic fibers and macroscopic rupture of alveolar walls (64–65).

Regarding the relative sensitivity of free lung DID in the current model; previous measurements of both free and total BALF DID were not significantly increased from control in animals treated with the same smoke and LPS regimen (66). While total lung DID levels were not measured in this model, previous studies from this laboratory

indicate that this parameter is even less sensitive than BALF DID for determining pulmonary elastic fiber injury, possibly due to concurrent repair of the fibers (65, 67).

4.4 Airspace Enlargement is Associated with Increased Elastin Crosslinking in Human Pulmonary Emphysema

The role of crosslinks in determining the mechanical and morphological characteristics of lung parenchyma was demonstrated by a study involving the use of beta-aminopropionitrile (BAPN), a crosslink inhibitor, to modify cadmium chloride-induced lung injury. Animals receiving this agent showed emphysematous changes in their lungs, whereas untreated animals developed interstitial fibrosis (70). Other studies have used crosslink inhibitors to induce airspace enlargement in different models of lung injury (71, 72). These findings provided additional evidence that DID might play an important role in the development of pulmonary emphysema.

In comparison to other proposed biomarkers, structural components such as DID may be better indicators of pulmonary emphysema than inflammatory mediators because they reflect emerging abnormalities in mechanical forces within the lung (60). However, the use of blood or urine levels of DID to determine the progression of COPD is complicated by the fact that both fluids contain elastic fiber breakdown products from sites other than the lung, including elastic fiber-rich tissues such as blood vessels and cartilage. Consequently, diseases such as arteriosclerosis or osteoarthritis may obscure the component of elastic fiber injury due to pulmonary emphysema.

To address this problem, our laboratory previously performed measurements of free DID released from lung elastic fibers following the use of cigarette smoke and lipopolysaccharide to induce pulmonary emphysema (69). The levels of free DID were

then correlated with airspace size, and the results supported the hypothesis that free lung DID may serve as a biomarker for airspace enlargement in pulmonary emphysema. While it is possible that post-mortem tissue autolysis could adversely affect the specificity of free lung DID, there was no correlation between tissue recovery time and free DID in the current study (Tables 12 and 13).

In contrast to free lung DID, the crosslink density in FFPE tissue sections provided a means of evaluating the repair process. Despite the fact that an undetermined amount of DID may be derived from fragmented elastic fibers with no structural significance, the presumptive abundance of intact fibers suggests that crosslink density may be a consistent measure of elastic fiber resynthesis and remodeling. By comparing this parameter with free DID levels in wet tissue it was possible to relate the breakdown and repair of elastic fibers to the progression of airspace enlargement in pulmonary emphysema.

Perhaps the most interesting finding was the increase in DID density in the lungs from COPD patients. Although previous investigations have shown that pulmonary emphysema is associated with either similar or decreased elastic fiber content compared to normal lungs, our results suggest that earlier stages of the disease may involve a more balanced relationship between injury and repair, where the damaging effects of inflammation and alveolar wall strain are offset by enhanced elastin crosslinking (64, 73-74). This mechanism may help maintain the normal movement of mechanical forces through the lung parenchyma during expansion and contraction and prevent alveolar wall distention.

The effect of the elastic fiber network on the distribution of these forces may be modeled by constructing a network of interconnecting units with two different levels of stiffness (K1 and K2), corresponding to either structurally weak or strong elastic fibers, respectively (75). The amount of mechanical deflection in response to a force is inversely proportional to the degree of stiffness. Therefore, K1 units are more prone to mechanical stretching than their stiffer counterparts.

To simulate elastic fiber injury, the two types of units are arranged randomly throughout a three-dimensional lattice representing the lung interstitium. Under these conditions, the percolation of mechanical forces through the lattice depends on the ratio of K1 to K2 (Figure 22). When there are few K1 units, percolation of mechanical forces is predominantly through K2, ensuring that there is little or no disruption of lung architecture. Conversely, when K1 units predominate, mechanical forces mainly percolate along the weaker pathways in the network, producing distortion of lung architecture. The ratio of K1 to K2 units is thus the critical determinant in modeling the emergence of pulmonary emphysema. The shift from a latent to an active state, characterized by changes in FEV1 and other parameters, is commonly referred to as a phase transition, and may be accompanied by a sudden change the physical behavior of the substrate in which this process occurs.

Applying this model to the lung, the K1 fibers would correspond to weakly crosslinked portions of elastic fibers whereas well-crosslinked regions would represent K2 fibers. In terms of breakdown products, the percolation of forces through the weakly crosslinked regions of elastin would cause greater distention of the peptide chains, increasing the likelihood of mechanical failure and breakage of chemical bonds. The

unraveling of these weakly crosslinked regions would presumably make them more susceptible to enzymatic breakdown, resulting in the release of smaller peptide fragments and individual DID crosslinks (76).

It is therefore hypothesized that the sudden increase in free DID at an MLI of 400 μm reflects a phase transition where the disease process enters an active state accompanied by alveolar wall rupture. The proposed emergence of significant disease at this point has important implications for therapeutic intervention. Prior to the phase transition, agents that prevent elastic fiber injury may succeed in shifting the balance between injury and repair in favor of restoring the structural integrity of alveolar walls. However, the potential efficacy of such treatment would be greatly reduced once the transition to alveolar wall rupture had occurred.

While the concept of phase transitions in the development of disease is not new, the investigation of these processes in the lung has been limited by the difficulty of relating specific biochemical events to morphological and physiological changes (62, 77-80). The current study provides a new approach to this problem, which has the potential to increase our understanding of the pathogenesis of pulmonary emphysema. As these types of investigations reveal critical changes in the microarchitecture of alveolar walls, it may be possible to identify a number of biomarkers that reflect the pattern of disease progression and may therefore serve as surrogate endpoints in clinical trials. The extreme sensitivity of mass spectrometry suggests that measurement of DID and other molecules in transbronchial biopsies could eventually become an accepted procedure for rapidly evaluating therapeutic agents, thereby facilitating the development of an effective treatment for COPD.

CHAPTER 5: CONCLUSION

We have successfully developed a new LC–MS-MS method for the quantification of DID in body fluids (plasma, urine) and tissues (sputum, lung). The method was then applied to an animal and human model of COPD. From this, we determined that free lung DID is a sensitive and specific indicator of alveolar wall injury in COPD. Our method has numerous advantages over previous methods of DID analysis which only permit quantification in less specific matrices (e.g. urine), where DID excretion may have occurred from other diseases involving elastin breakdown as a pathogenic mechanism. Using this research, it may be possible to produce a topological map of the lung relating localized alveolar wall changes with the loss of elastin crosslinks, thereby revealing a pattern of disease progression in pulmonary emphysema.

The ability to accurately measure elastic fiber injury in both fresh and formalin-fixed tissue will help increase our understanding of the pathogenesis of pulmonary emphysema. Nevertheless, determining the relative usefulness of free lung DID as a means of quantifying alveolar wall injury will require additional testing in a variety of animal models of pulmonary emphysema as well as in additional human autopsy specimens. DID measurements taken from lung specimens derived from a variety of pulmonary diseases including cystic fibrosis, lung cancer, and acute respiratory distress syndrome would also provide a wealth of additional information with respect to the progression of these particular diseases, which may vary significantly. The analysis of postmortem tissue presents additional analytical and interpretive challenges, whereby

autolysis due to delayed formalin fixation may result in the additional release of free DID which might adversely affect its specificity. Furthermore, the accuracy and reproducibility of the described LC–MS-MS procedure will need to be confirmed by multiple independent laboratories. The development of a commonly accepted protocol involving the use of a specific internal standard would facilitate this process.

DID as a biomarker of disease can be utilized further to monitor the efficacy of potential therapeutic agents used in the treatment of pulmonary emphysema. Previous studies have utilized plasma and urine for this purpose (17, 37), but such fluids may not be specific to lung disease owing to the presence of other comorbidities (hypertension, heart disease, atherosclerosis, etc.) where elastic fiber degradation is a central pathophysiologic mechanism. Sputum is an alternative matrix that may be more specific to the lung. However, sufficient quantities of sputum are often difficult to acquire, thereby limiting its reproducibility as a specimen of choice. As the current study was limited to postmortem animal or human lung tissue for DID analysis, its current application to living patients is limited. In this regard, determining free DID content in either transbronchial or CT-guided biopsies may be a more reliable alternative to sputum or less specific body fluids.

The fact that suspension of lung tissue in formalin did not remove free DID from tissues suggest that the crosslinks might become attached to other molecules that undergo fixation. One study indicates that DID may bind to fatty acids through electrostatic interactions involving the positively charged quaternary ammonium group of the crosslinks (68). These attachments might then be abolished during the chromatographic phase of DID analysis, allowing separation and measurement of these crosslinks.

While further work is needed to validate the use of free DID as a biomarker for pulmonary emphysema, the ability to accurately measure elastic fiber injury in fresh and formalin-fixed lung tissue would increase our understanding of the pathogenesis of pulmonary emphysema. Taking this process one step further, it may be possible to produce a topological map of the lung relating localized alveolar wall changes with the loss of elastin crosslinks, thereby revealing the pattern of disease progression in pulmonary emphysema.

REFERENCES

1. Definition and classification of chronic bronchitis for clinical and epidemiological purposes. A report to the Medical Research Council by their Committee on the Aetiology of Chronic Bronchitis. *Lancet*. 1965 Apr 10;1(7389):775-9. PMID: 4165081.
2. Fletcher CM, Pride NB. Definitions of emphysema, chronic bronchitis, asthma, and airflow obstruction: 25 years on from the Ciba symposium. *Thorax*. 1984 Feb;39(2):81-5. doi: 10.1136/thx.39.2.81. PMID: 6701830; PMCID: PMC459731.
3. L. Reid, *The pathology of emphysema*, Chicago: Year Book Medical Publishers; 1967.
4. Mitzner W. Emphysema--a disease of small airways or lung parenchyma? *N Engl J Med*. 2011 Oct 27;365(17):1637-9. doi: 10.1056/NEJMe1110635. PMID: 22029986; PMCID: PMC4565515.
5. Goptu B, Ekeowa UI, Lomas DA. Mechanisms of emphysema in alpha1-antitrypsin deficiency: molecular and cellular insights. *Eur Respir J*. 2009 Aug;34(2):475-88. doi: 10.1183/09031936.00096508. PMID: 19648523.
6. Imboden M, Bouzigon E, Curjuric I, Ramasamy A, Kumar A, Hancock DB, Wilk JB, Vonk JM, Thun GA, Siroux V, Nadif R, Monier F, Gonzalez JR, Wjst M, Heinrich J, Loehr LR, Franceschini N, North KE, Altmüller J, Koppelman GH, Guerra S,

Kronenberg F, Lathrop M, Moffatt MF, O'Connor GT, Strachan DP, Postma DS, London SJ, Schindler C, Kogevinas M, Kauffmann F, Jarvis DL, Demenais F, Probst-Hensch NM. Genome-wide association study of lung function decline in adults with and without asthma. *J Allergy Clin Immunol*. 2012 May;129(5):1218-28. doi: 10.1016/j.jaci.2012.01.074. Epub 2012 Mar 16. PMID: 22424883; PMCID: PMC3340499.

7. Eisner MD, Anthonisen N, Coultas D, Kuenzli N, Perez-Padilla R, Postma D, Romieu I, Silverman EK, Balmes JR; Committee on Nonsmoking COPD, Environmental and Occupational Health Assembly. An official American Thoracic Society public policy statement: Novel risk factors and the global burden of chronic obstructive pulmonary disease. *Am J Respir Crit Care Med*. 2010 Sep 1;182(5):693-718. doi: 10.1164/rccm.200811-1757ST. PMID: 20802169.

8. Laniado-Laborín R. Smoking and chronic obstructive pulmonary disease (COPD). Parallel epidemics of the 21 century. *Int J Environ Res Public Health*. 2009 Jan;6(1):209-24. doi: 10.3390/ijerph6010209. Epub 2009 Jan 9. PMID: 19440278; PMCID: PMC2672326.

9. Sharma, A., Pitchforth, D., Richards, G., & Barclay, J. (2010). *COPD in Primary Care* (1st ed.). CRC Press. <https://doi.org/10.4324/9781315379043>

10. Hu G, Zhou Y, Tian J, Yao W, Li J, Li B, Ran P. Risk of COPD from exposure to biomass smoke: a metaanalysis. *Chest*. 2010 Jul;138(1):20-31. doi: 10.1378/chest.08-2114. Epub 2010 Feb 5. PMID: 20139228.
11. Shapiro SD, Ingenito EP. The pathogenesis of chronic obstructive pulmonary disease: advances in the past 100 years. *Am J Respir Cell Mol Biol*. 2005 May;32(5):367-72. doi: 10.1165/rcmb.F296. PMID: 15837726.
12. Laurell CB, Eriksson S. The electrophoretic α 1-globulin pattern of serum in α 1-antitrypsin deficiency. 1963. *COPD*. 2013 Mar;10 Suppl 1:3-8. doi: 10.3109/15412555.2013.771956. PMID: 23527532.
13. Houghton AM. Endogenous modifiers of cigarette smoke exposure within the lung. *Proc Am Thorac Soc*. 2012 May;9(2):66-8. doi: 10.1513/pats.201108-046MS. PMID: 22550246; PMCID: PMC3359106.
14. Atkinson JJ, Senior RM. Matrix metalloproteinase-9 in lung remodeling. *Am J Respir Cell Mol Biol*. 2003 Jan;28(1):12-24. doi: 10.1165/rcmb.2002-0166TR. PMID: 12495928.
15. Pesci A, Balbi B, Majori M, Cacciani G, Bertacco S, Alciato P, Donner CF. Inflammatory cells and mediators in bronchial lavage of patients with chronic obstructive

pulmonary disease. *Eur Respir J*. 1998 Aug;12(2):380-6. doi:
10.1183/09031936.98.12020380. PMID: 9727789.

16. Braber S, Thio M, Blokhuis BR, Henricks PA, Koelink PJ, Groot Kormelink T, Bezemer GF, Kerstjens HA, Postma DS, Garssen J, Kraneveld AD, Redegeld FA, Folkerts G. An association between neutrophils and immunoglobulin free light chains in the pathogenesis of chronic obstructive pulmonary disease. *Am J Respir Crit Care Med*. 2012 Apr 15;185(8):817-24. doi: 10.1164/rccm.201104-0761OC. Epub 2012 Jan 6. PMID: 22227380.

17. Cantor JO, Ma S, Liu X, Campos MA, Strange C, Stocks JM, Devine MS, El Bayadi SG, Lipchik RJ, Sandhaus RA, Turino GM. A 28-day clinical trial of aerosolized hyaluronan in alpha-1 antiprotease deficiency COPD using desmosine as a surrogate marker for drug efficacy. *Respir Med*. 2021 Jun;182:106402. doi:
10.1016/j.rmed.2021.106402. Epub 2021 Apr 14. PMID: 33906126.

18. Thomsen M, Dahl M, Lange P, Vestbo J, Nordestgaard BG. Inflammatory biomarkers and comorbidities in chronic obstructive pulmonary disease. *Am J Respir Crit Care Med*. 2012 Nov 15;186(10):982-8. doi: 10.1164/rccm.201206-1113OC. Epub 2012 Sep 13. PMID: 22983959.

19. Gordon C, Gudi K, Krause A, Sackrowitz R, Harvey BG, Strulovici-Barel Y, Mezey JG, Crystal RG. Circulating endothelial microparticles as a measure of early lung

destruction in cigarette smokers. *Am J Respir Crit Care Med*. 2011 Jul 15;184(2):224-32. doi: 10.1164/rccm.201012-2061OC. Epub 2011 Mar 11. PMID: 21471087; PMCID: PMC3172886.

20. Cazzola M, MacNee W, Martinez FJ, Rabe KF, Franciosi LG, Barnes PJ, Brusasco V, Burge PS, Calverley PM, Celli BR, Jones PW, Mahler DA, Make B, Miravittles M, Page CP, Palange P, Parr D, Pistolesi M, Rennard SI, Rutten-van Mülken MP, Stockley R, Sullivan SD, Wedzicha JA, Wouters EF; American Thoracic Society; European Respiratory Society Task Force on outcomes of COPD. Outcomes for COPD pharmacological trials: from lung function to biomarkers. *Eur Respir J*. 2008 Feb;31(2):416-69. doi: 10.1183/09031936.00099306. PMID: 18238951.

21. De Gruttola VG, Clax P, DeMets DL, Downing GJ, Ellenberg SS, Friedman L, Gail MH, Prentice R, Wittes J, Zeger SL. Considerations in the evaluation of surrogate endpoints in clinical trials. summary of a National Institutes of Health workshop. *Control Clin Trials*. 2001 Oct;22(5):485-502. doi: 10.1016/s0197-2456(01)00153-2. PMID: 11578783.

22. Ma S, Lin YY, Tartell L, Turino GM. The effect of tiotropium therapy on markers of elastin degradation in COPD. *Respir Res*. 2009 Feb 25;10(1):12. doi: 10.1186/1465-9921-10-12. PMID: 19243601; PMCID: PMC2682791.

23. Partridge SM, Elsdon DF, Thomas J. Constitution of the cross-linkages in elastin. *Nature*. 1963 Mar 30;197:1297-8. doi: 10.1038/1971297a0. PMID: 13941623.
24. Viglio S, Annovazzi L, Luisetti M, Stolk J, Casado B, Iadarola P. Progress in the methodological strategies for the detection in real samples of desmosine and isodesmosine, two biological markers of elastin degradation. *J Sep Sci*. 2007 Feb;30(2):202-13. doi: 10.1002/jssc.200600260. PMID: 17390614.
25. J. Cody, S.P. Vorce, *Principles of Forensic Toxicology*, AACC Press, Washington DC, 2010 (4th ed.), pp. 141–161.
26. Agilent Technologies Inc., 6100 concepts guide (2017) 1-120. https://www.agilent.com/cs/library/usermanuals/public/G1960-90104_ChemStation_ConceptsGuide.pdf (Accessed Feb 5th, 2021).
27. Fagiola M. Current and future directions of high resolution and tandem mass spectrometry in postmortem and human performance toxicology. *Leg Med (Tokyo)*. 2019 Mar;37:86-94. doi: 10.1016/j.legalmed.2019.02.004. Epub 2019 Feb 16. PMID: 30797132.
28. Knudsen L, Weibel ER, Gundersen HJ, Weinstein FV, Ochs M. Assessment of air space size characteristics by intercept (chord) measurement: an accurate and efficient

stereological approach. *J Appl Physiol* (1985). 2010 Feb;108(2):412-21. doi: 10.1152/jappphysiol.01100.2009. Epub 2009 Dec 3. PMID: 19959763.

29. Hsiao JJ, Potter OG, Chu TW, Yin H. Improved LC/MS Methods for the Analysis of Metal-Sensitive Analytes Using Medronic Acid as a Mobile Phase Additive. *Anal Chem*. 2018 Aug 7;90(15):9457-9464. doi: 10.1021/acs.analchem.8b02100. Epub 2018 Jul 18. PMID: 29976062.

30. Ma S, Lin YY, Turino GM. Measurements of desmosine and isodesmosine by mass spectrometry in COPD. *Chest*. 2007 May;131(5):1363-71. doi: 10.1378/chest.06-2251. PMID: 17494786.

31. Ma S, Turino GM, Lin YY. Quantitation of desmosine and isodesmosine in urine, plasma, and sputum by LC-MS/MS as biomarkers for elastin degradation. *J Chromatogr B Analyt Technol Biomed Life Sci*. 2011 Jul 1;879(21):1893-8. doi: 10.1016/j.jchromb.2011.05.011. Epub 2011 May 13. PMID: 21621489.

32. Shiraishi K, Matsuzaki K, Matsumoto A, Hashimoto Y, Iba K. Development of a robust LC-MS/MS method for determination of desmosine and isodesmosine in human urine. *J Oleo Sci*. 2010;59(8):431-9. doi: 10.5650/jos.59.431. PMID: 20625235.

33. Huang JT, Chaudhuri R, Albarbarawi O, Barton A, Grierson C, Rauchhaus P, Weir CJ, Messow M, Stevens N, McSharry C, Feuerstein G, Mukhopadhyay S, Brady J,

Palmer CN, Miller D, Thomson NC. Clinical validity of plasma and urinary desmosine as biomarkers for chronic obstructive pulmonary disease. *Thorax*. 2012 Jun;67(6):502-8. doi: 10.1136/thoraxjnl-2011-200279. Epub 2012 Jan 16. PMID: 22250098; PMCID: PMC3358730.

34. Albarbarawi O, Barton A, Lin Z, Takahashi E, Buddharaju A, Brady J, Miller D, Palmer CN, Huang JT. Measurement of urinary total desmosine and isodesmosine using isotope-dilution liquid chromatography-tandem mass spectrometry. *Anal Chem*. 2010 May 1;82(9):3745-50. doi: 10.1021/ac100152f. PMID: 20361748.

35. AAFS Standards Board (2019) Standard Practices for Method Validation in Forensic Toxicology. ANSI/ASB Standard 036, First Edition.
http://www.asbstandardsboard.org/wp-content/uploads/2019/11/036_Std_e1.pdf

36. Stone PJ, Gottlieb DJ, O'Connor GT, Ciccolella DE, Breuer R, Bryan-Rhadfi J, Shaw HA, Franzblau C, Snider GL. Elastin and collagen degradation products in urine of smokers with and without chronic obstructive pulmonary disease. *Am J Respir Crit Care Med*. 1995 Apr;151(4):952-9. doi: 10.1164/ajrccm.151.4.7697272. PMID: 7697272.

37. Cantor J, Ma S, Turino G. A pilot clinical trial to determine the safety and efficacy of aerosolized hyaluronan as a treatment for COPD. *Int J Chron Obstruct Pulmon Dis*. 2017 Sep 18;12:2747-2752. doi: 10.2147/COPD.S142156. PMID: 29075107; PMCID: PMC5609793.

38. Ma S, Lin YY, He J, Rouhani FN, Brantly M, Turino GM. Alpha-1 antitrypsin augmentation therapy and biomarkers of elastin degradation. *COPD*. 2013 Aug;10(4):473-81. doi: 10.3109/15412555.2013.771163. Epub 2013 Apr 5. PMID: 23560990.
39. Ma S, Lin YY, Cantor JO, Chapman KR, Sandhaus RA, Fries M, Edelman JM, McElvaney G, Turino GM. The Effect of Alpha-1 Proteinase Inhibitor on Biomarkers of Elastin Degradation in Alpha-1 Antitrypsin Deficiency: An Analysis of the RAPID/RAPID Extension Trials. *Chronic Obstr Pulm Dis*. 2016 Nov 18;4(1):34-44. doi: 10.15326/jcopdf.4.1.2016.0156. PMID: 28848909; PMCID: PMC5560248.
40. Turino GM, Lin YY, He J, Cantor JO, Ma S. Elastin degradation: an effective biomarker in COPD. *COPD*. 2012 Aug;9(4):435-8. doi: 10.3109/15412555.2012.697753. Epub 2012 Jun 26. PMID: 22734624.
41. Murakami Y, Suzuki R, Yanuma H, He J, Ma S, Turino GM, Lin YY, Usuki T. Synthesis and LC-MS/MS analysis of desmosine-CH₂, a potential internal standard for the degraded elastin biomarker desmosine. *Org Biomol Chem*. 2014 Dec 28;12(48):9887-94. doi: 10.1039/c4ob01438c. PMID: 25355397.
42. Albarbarawi O, Barton A, Miller D, McSharry C, Chaudhuri R, Thomson NC, Palmer CN, Devereux G, Huang JT. Characterization and validation of an isotope-dilution LC-

MS/MS method for quantification of total desmosine and isodesmosine in plasma and serum. *Bioanalysis*. 2013 Aug;5(16):1991-2001. doi: 10.4155/bio.13.164. PMID: 23937134.

43. Ma S, Lieberman S, Turino GM, Lin YY. The detection and quantitation of free desmosine and isodesmosine in human urine and their peptide-bound forms in sputum. *Proc Natl Acad Sci U S A*. 2003 Oct 28;100(22):12941-3. doi: 10.1073/pnas.2235344100. Epub 2003 Oct 16. PMID: 14563926; PMCID: PMC240723.

44. Bush, D.R.; *The LC/MS/MS Analysis of Pyridinoline and Desmosines in Hypertensive Mouse Aorta, Elucidation of Arginine and Proline Fragmentation for the Analysis of Arginine Metabolism in Mosquitoes by LC/MS/MS, and Mudpit Identification of B. Pseudomallei Proteins in Urine*; University of Arizona, (2013); <https://repository.arizona.edu/handle/10150/293615> (accessed January 19th, 2022).

45. Black D, Duncan A, Robins SP. Quantitative analysis of the pyridinium crosslinks of collagen in urine using ion-paired reversed-phase high-performance liquid chromatography. *Anal Biochem*. 1988 Feb 15;169(1):197-203. doi: 10.1016/0003-2697(88)90274-6. PMID: 3369682.

46. Chen JR, Takahashi M, Kushida K, Suzuki M, Suzuki K, Horiuchi K, Nagano A. Direct detection of crosslinks of collagen and elastin in the hydrolysates of human yellow

ligament using single-column high performance liquid chromatography. *Anal Biochem.* 2000 Feb 15;278(2):99-105. doi: 10.1006/abio.1999.4412. PMID: 10660450.

47. Saito M, Marumo K, Fujii K, Ishioka N. Single-column high-performance liquid chromatographic-fluorescence detection of immature, mature, and senescent cross-links of collagen. *Anal Biochem.* 1997 Nov 1;253(1):26-32. doi: 10.1006/abio.1997.2350. PMID: 9356137.

48. Salomoni M, Muda M, Zuccato E, Mussini E. High-performance liquid chromatographic determination of desmosine and isodesmosine after phenylisothiocyanate derivatization. *J Chromatogr.* 1991 Dec 6;572(1-2):312-6. doi: 10.1016/0378-4347(91)80496-y. PMID: 1818066.

49. Cumiskey WR, Pagani ED, Bode DC. Enrichment and analysis of desmosine and isodesmosine in biological fluids. *J Chromatogr B Biomed Appl.* 1995 Jun 23;668(2):199-207. doi: 10.1016/0378-4347(95)00092-w. PMID: 7581855.

50. Zhang J, Raglione T, Wang Q, Kleintop B, Tomasella F, Liang X. Regeneration of tetrabutylammonium ion-pairing reagent distribution in a gradient elution of reversed phase ion-pair chromatography. *J Chromatogr Sci.* 2011 Nov-Dec;49(10):825-31. doi: 10.1093/chrsi/49.10.825. PMID: 22080812.

51. Zarate E, Boyle V, Rupprecht U, Green S, Villas-Boas SG, Baker P, Pinu FR. Fully Automated Trimethylsilyl (TMS) Derivatisation Protocol for Metabolite Profiling by GC-MS. *Metabolites*. 2016 Dec 29;7(1):1. doi: 10.3390/metabo7010001. PMID: 28036063; PMCID: PMC5372204.
52. Thomas J, Elsdon DF, Partridge SM. Partial Structure of Two Major Degradation Products From The Cross-Linkages in Elastin. *Nature*. 1963 Nov 16;200:651-2. doi: 10.1038/200651a0. PMID: 14109938.
53. Luisetti M, Stolk J, Iadarola P. Desmosine, a biomarker for COPD: old and in the way. *Eur Respir J*. 2012 Apr;39(4):797-8. doi: 10.1183/09031936.00172911. PMID: 22467719.
54. Ma S, Turino GM, Hayashi T, Yanuma H, Usuki T, Lin YY. Stable deuterium internal standard for the isotope-dilution LC-MS/MS analysis of elastin degradation. *Anal Biochem*. 2013 Sep 15;440(2):158-65. doi: 10.1016/j.ab.2013.05.014. Epub 2013 May 30. PMID: 23727558.
55. Kulkarni GS, Nadkarni PP, Cerreta JM, Ma S, Cantor JO. Short-term cigarette smoke exposure potentiates endotoxin-induced pulmonary inflammation. *Exp Lung Res*. 2007 Jan-Feb;33(1):1-13. doi: 10.1080/01902140601112957. PMID: 17364908.

56. Moerloose KB, Pauwels RA, Joos GF. Short-term cigarette smoke exposure enhances allergic airway inflammation in mice. *Am J Respir Crit Care Med*. 2005 Jul 15;172(2):168-72. doi: 10.1164/rccm.200409-1174OC. Epub 2005 Apr 14. PMID: 15831841.
57. Van der Vaart H, Postma DS, Timens W, ten Hacken NH. Acute effects of cigarette smoke on inflammation and oxidative stress: a review. *Thorax*. 2004 Aug;59(8):713-21. doi: 10.1136/thx.2003.012468. PMID: 15282395; PMCID: PMC1747102.
58. Hoidal JR, Niewoehner DE. Cigarette smoke inhalation potentiates elastase-induced emphysema in hamsters. *Am Rev Respir Dis*. 1983 Apr;127(4):478-81. doi: 10.1164/arrd.1983.127.4.478. PMID: 6551161.
59. Shapiro SD, Goldstein NM, Houghton AM, Kobayashi DK, Kelley D, Belaaouaj A. Neutrophil elastase contributes to cigarette smoke-induced emphysema in mice. *Am J Pathol*. 2003 Dec;163(6):2329-35. doi: 10.1016/S0002-9440(10)63589-4. PMID: 14633606; PMCID: PMC1892384.
60. Doyle TJ, Pinto-Plata V, Morse D, Celli BR, Rosas IO. The expanding role of biomarkers in the assessment of smoking-related parenchymal lung diseases. *Chest*. 2012 Oct;142(4):1027-1034. doi: 10.1378/chest.12-1540. PMID: 23032451; PMCID: PMC3465104.

61. Rosenberg SR, Kalhan R. Biomarkers in chronic obstructive pulmonary disease. *Transl Res.* 2012 Apr;159(4):228-37. doi: 10.1016/j.trsl.2012.01.019. Epub 2012 Feb 7. PMID: 22424427.
62. Suki B, Bates JH. Lung tissue mechanics as an emergent phenomenon. *J Appl Physiol* (1985). 2011 Apr;110(4):1111-8. doi: 10.1152/jappphysiol.01244.2010. Epub 2011 Jan 6. PMID: 21212247; PMCID: PMC3075131.
63. Bates JH, Davis GS, Majumdar A, Butnor KJ, Suki B. Linking parenchymal disease progression to changes in lung mechanical function by percolation. *Am J Respir Crit Care Med.* 2007 Sep 15;176(6):617-23. doi: 10.1164/rccm.200611-1739OC. Epub 2007 Jun 15. PMID: 17575096; PMCID: PMC1994222.
64. Deslee G, Woods JC, Moore CM, Liu L, Conradi SH, Milne M, Gierada DS, Pierce J, Patterson A, Lewit RA, Battaile JT, Holtzman MJ, Hogg JC, Pierce RA. Elastin expression in very severe human COPD. *Eur Respir J.* 2009 Aug;34(2):324-331. doi: 10.1183/09031936.00123008. Epub 2009 Apr 8. PMID: 19357152; PMCID: PMC3758126.
65. Mehraban S, Gu G, Ma S, Liu X, Turino G, Cantor J. The proinflammatory activity of structurally altered elastic fibers. *Am J Respir Cell Mol Biol.* 2020 Nov;63(5):699-706. doi: 10.1165/rcmb.2020-0064OC. PMID: 32790529.

66. Gu, G., 2021. Short-term second-hand smoke exposure predisposes the lung to inflammation, elastic fiber injury, and pulmonary emphysema. St John's University Theses and Dissertations. pp 1-72. https://scholar.stjohns.edu/theses_dissertations/297.
67. Cantor J, Ochoa A, Ma S, Liu X, Turino G. Free Desmosine is a Sensitive Marker of Smoke-Induced Emphysema. *Lung*. 2018 Dec;196(6):659-663. doi: 10.1007/s00408-018-0163-1. Epub 2018 Sep 14. PMID: 30218154.
68. Vreeswijk, J. van (1995). Interaction between fatty acid and the elastin network. Thesis Wageningen. ISBN 90-5485-444-8 pp 1-94.
69. Fagiola M, Gu G, Avella J, Cantor J. Free lung desmosine: a potential biomarker for elastic fiber injury in pulmonary emphysema. *Biomarkers*. 2022 Jun;27(4):319-324. doi: 10.1080/1354750X.2022.2043443. Epub 2022 Feb 24. PMID: 35170389.
70. Niewoehner DE, Hoidal JR. Lung fibrosis and emphysema: divergent responses to a common injury? *Science*. 1982 Jul 23;217(4557):359-60. doi: 10.1126/science.7089570. PMID: 7089570.
71. Riley DJ, Kramer MJ, Kerr JS, Chae CU, Yu SY, Berg RA. Damage and repair of lung connective tissue in rats exposed to toxic levels of oxygen. *Am Rev Respir Dis*. 1987 Feb;135(2):441-7. doi: 10.1164/arrd.1987.135.2.441. PMID: 3813207.

72. Kuhn C 3rd, Starcher BC. The effect of lathyrogens on the evolution of elastase-induced emphysema. *Am Rev Respir Dis*. 1980 Sep;122(3):453-60. doi: 10.1164/arrd.1980.122.3.453. PMID: 6106444.

73. Black PN, Ching PS, Beaumont B, Ranasinghe S, Taylor G, Merrilees MJ. Changes in elastic fibres in the small airways and alveoli in COPD. *Eur Respir J*. 2008 May;31(5):998-1004. doi: 10.1183/09031936.00017207. Epub 2008 Jan 23. PMID: 18216063.

74. Merrilees MJ, Ching PS, Beaumont B, Hinek A, Wight TN, Black PN. Changes in elastin, elastin binding protein and versican in alveoli in chronic obstructive pulmonary disease. *Respir Res*. 2008 May 18;9(1):41. doi: 10.1186/1465-9921-9-41. PMID: 18485243; PMCID: PMC2397404.

75. K. D. Murphy, G. W. Hunt & D. P. Almond (2006) Evidence of emergent scaling in mechanical systems, *Philosophical Magazine*, 86:21-22, 3325-3338, DOI: 10.1080/14786430500197934

76. Jesudason R, Black L, Majumdar A, Stone P, Suki B. Differential effects of static and cyclic stretching during elastase digestion on the mechanical properties of extracellular matrices. *J Appl Physiol* (1985). 2007 Sep;103(3):803-11. doi: 10.1152/jappphysiol.00057.2007. Epub 2007 May 31. PMID: 17540839.

77. Clark AR, Kumar H, Burrowes K. Capturing complexity in pulmonary system modelling. *Proc Inst Mech Eng H*. 2017 May;231(5):355-368. doi: 10.1177/0954411916683221. PMID: 28427314.
78. Sturmberg JP. Multimorbidity and chronic disease: an emergent perspective. *J Eval Clin Pract*. 2014 Aug;20(4):508-12. doi: 10.1111/jep.12126. Epub 2014 Apr 5. PMID: 24702685.
79. Bates JH, Davis GS, Majumdar A, Butnor KJ, Suki B. Linking parenchymal disease progression to changes in lung mechanical function by percolation. *Am J Respir Crit Care Med*. 2007 Sep 15;176(6):617-23. doi: 10.1164/rccm.200611-1739OC. Epub 2007 Jun 15. PMID: 17575096; PMCID: PMC1994222.
80. Winkler T, Suki B. Emergent structure-function relations in emphysema and asthma. *Crit Rev Biomed Eng*. 2011;39(4):263-80. doi: 10.1615/critrevbiomedeng.v39.i4.20. PMID: 22011233; PMCID: PMC3228247.

Vita

Name	<i>Michael Fagiola</i>
Baccalaureate Degree	<i>Bachelor of Science, Shepherd University, Shepherdstown, WV Major: Chemistry – Biochemistry</i>
Date Graduated	<i>May, 2015</i>
Other Degrees and Certificates	<i>Master of Science, University of Florida, Gainesville, FL Major: Veterinary Medical Sciences – Forensic Toxicology</i>
Date Graduated	<i>December, 2018</i>